

**INDUCTION COOKER DESIGN AND EXPERIMENTAL RESULTS**  
**WITH QUASI RESONANT TOPOLOGY AND JITTER METHOD**

A Thesis  
by  
Mehmet Emin Tülü

Submitted to the  
Graduate School of Sciences and Engineering  
In Partial Fulfillment of the Requirements for  
the Degree of  
Master of Science  
in the  
Department of Electrical and Electronics Engineering

Özyeğin University  
August 2012

Copyright © 2012 by Mehmet Emin Tülü

**INDUCTION COOKER DESIGN AND EXPERIMENTAL RESULTS**  
**WITH QUASI RESONANT TOPOLOGY AND JITTER METHOD**

Approved by:

---

Asst. Prof. Deniz Yıldırım, Advisor  
Department of Electrical  
Engineering  
*İstanbul Technical University*

---

Asst. Prof. H. Fatih Uğurdağ, Advisor  
Department of Electrical and  
Electronics Engineering  
*Özyeğin University*

---

Associate Prof. Oğuz Sunay  
Department of Electrical and  
Electronics Engineering  
*Özyeğin University*

---

Associate Prof. Murat Uysal  
Department of Electrical and  
Electronics Engineering  
*Özyeğin University*

Date Approved: \_\_ September 2012

---

Associate Prof. Mehmet Arık  
Department of Mechanical  
Engineering  
*Özyeğin University*

*To My Family...*

*Metin Tülü, Memnune Tülü,*

*Güzin Tülü, and Esin Tülü*

## ABSTRACT

This thesis presents an induction cooker design and its detailed experimental results. The design is based on Quasi Resonant Topology and is unique in terms of the particular Jitter Method it employs to drive the semiconductor switches (IGBTs).

Most induction cookers are based on Half Bridge Topology. Although Quasi Resonant Topology offers a more cost effective implementation, it introduces more EMI problems. However, we solve these problems with our Jitter Method. Although there are other works in the literature that solve the EMI issues by some sort of jitter methods (i.e., spread spectrum methods), these methods do not address the high voltage stress created across the IGBTs. However, the Jitter Method proposed in this thesis also reduces collector-emitter voltage stress besides improving EMI. Note that jitter methods also prevent mechanical vibration (i.e., resonance), which cause audible noise.

Another thing that makes this thesis unique in the literature is the rich set of experimental results it contains – based on an experimental prototype we built with a power rating of 2300W. While the existing literature mostly contains theoretical treatment, we have produced detailed experimental results for Quasi Resonant Topology and show that the current harmonics (drawn from the utility) stay within the published standards (TS EN 61000-3-2). We also include experimental results for Delivered Power Detection, Pan Detection, and Protection Circuits.

In addition to what is listed above, this thesis also goes over some theory and explains electromagnetic induction, skin effect, switching action, and resonant converters in order to provide a clear understanding of induction cookers. It also covers the fundamentals of Quasi Resonant and Half Bridge topologies. These two topologies are compared on the basis of electromagnetic compatibility, cost, and applicability. Moreover, control and protection issues that guarantee stable working modes for the cooker are covered such as protection circuits for abnormal conditions, requirements for soft start, and a method for pan detection. Among other things, we also discuss methods that determine power delivered to the pan.

## ÖZETÇE

Bu tezde, indüksiyon ocak tasarımı ve detaylı deneysel sonuçları sunulmaktadır. Tasarım Yarı Rezonans Yapıya dayanır ve yarı iletken anahtarları sürmek için kullanılan özel Yayılmış Tayf yöntemi ile literatürde özgün bir yere sahiptir.

Birçok indüksiyon ocak tasarımında Yarı Köprü yapısı kullanılır. Yarı Rezonans yapısı maliyet olarak daha avantajlı olmasına rağmen, bu yapının elektromanyetik yayılımı daha yüksektir. Ancak, bu problem tezde Yayılmış Tayf Metodu ile çözülmektedir. Literatürde değişik şekillerde yapılmış Yayılmış Tayf Yöntemleri elektromanyetik yayılım problemini çözerken, yarı iletken anahtar üzerindeki yüksek voltaj konusunda bir çözüm üretilmemektedir. Ancak, bu tezde anlatılan Yayılmış Tayf Yöntemi, EMI sorunlarını çözerken, yarı iletken (IGBT) üzerindeki yüksek voltaj problemini de çözmektedir. Not edilmelidir ki, tüm jitter yöntemleri rezonans durumunda oluşacak olan mekanik titreşme problemlerini ve dolayısıyla duyulabilir gürültü problemini de çözer.

Bu tezi literatürde özgün kılan başka bir nokta ise zengin deneysel sonuçlar barındırmasıdır ki bu ölçümler 2300W gücünde hazırlanan bir prototip üzerinden alınmıştır. Bu konudaki literatür çalışmaları genel olarak teorik konulara değinirken, tezde detaylı Yarı Rezonans Yapı deneysel sonuçları yer almakta ve şebekeden çekilen akım harmoniklerinin standartlar (TS EN 61000-3-2) içinde olduğu gösterilmiştir. Ayrıca aktarılan güç hesabı, tencere algılama ve koruma devreleri konusunda da deneysel sonuçlar paylaşılmaktadır.

Üstte listelenenlere ek olarak, indüksiyon ocak tasarımının anlaşılabilmesi için teori üzerinden gidilerek elektromanyetik indüksiyon, deri etkisi, anahtarlama işlemi ve rezonans çeviriciler konuları açıklanmıştır. Ayrıca Yarı Köprü ve Yarı Rezonans yapıları temel olarak anlatılmaktadır. Bu iki yapı, elektromanyetik uyumluluk, maliyet ve uygulanabilirlik açısından karşılaştırılmıştır. Ayrıca, anormal durumlar için koruma devreleri, yumuşak başlangıç gerekliliği ve tencere algılama metodu gibi ocağın dayanıklı biçimde çalışmasını garanti eden koruma ve kontrol devreleri işlenmektedir. Bunlara ek olarak, tencereye aktarılan gücün miktarının anlaşılabilmesi için yöntemler anlatılmaktadır.

## **ACKNOWLEDGEMENTS**

It was a great experience to work with my advisors Asst. Prof. Deniz YILDIRIM and Asst. Prof. H. Fatih UĞURDAĞ throughout my thesis. I thank them for their contribution to this work.

I also thank my colleagues Mr. Cengiz Tarhan and Mr. H. Cem Kızıları for their encouragement and support throughout this work in the laboratories of VESTEL Electronics.

Last but not least, I am grateful to my family and thank them for all they have done for me so far.

**August 2012**

**Mehmet Emin TÖLÜ**

# TABLE OF CONTENTS

<b>DEDICATION.....</b>	<b>iii</b>
<b>ABSTRACT.....</b>	<b>iv</b>
<b>ÖZETÇE.....</b>	<b>v</b>
<b>ACKNOWLEDGEMENTS.....</b>	<b>vi</b>
<b>ABBREVIATIONS.....</b>	<b>ix</b>
<b>LIST OF TABLES.....</b>	<b>x</b>
<b>LIST OF FIGURES.....</b>	<b>xi</b>
<b>LIST OF SYMBOLS.....</b>	<b>xiii</b>
<b>I. INTRODUCTION.....</b>	<b>1</b>
1.1 Description of Induction Cooker.....	1
1.2 Basics of Induction Heating.....	3
1.2.1 The Fundamental Theory.....	3
1.2.2 Electromagnetic Induction.....	4
1.2.3 The Skin Effect.....	5
1.3 Induction Cooker System Features.....	6
1.4 Previous Work.....	8
1.5 Contributions of This Thesis.....	10
<b>II. DESIGN AND ANALYSIS.....</b>	<b>11</b>
2.1 Theory.....	11
2.1.1 Switching Action.....	11
2.1.2 Resonant Converter.....	13
2.2 Quasi Resonant Topology (QRT).....	16
2.3 Half Bridge Topology and Comparison to QRT.....	20
<b>III. JITTER METHOD.....</b>	<b>23</b>
<b>IV. EXPERIMENTAL RESULTS.....</b>	<b>29</b>
4.1 Results for QRT.....	29
4.2 Efficiency Measurement and Uncertainty Analysis.....	40
4.3 Control and Protection Issues.....	41
4.3.1 Delivered Power Detection.....	41
4.3.2 Pan Detection.....	45

4.3.3 Protection Circuits.....	47
<b>V. CONCLUSIONS and FUTURE WORK .....</b>	<b>54</b>
<b>REFERENCES.....</b>	<b>56</b>
<b>VITA.....</b>	<b>59</b>



## ABBREVIATIONS

<b>SMPS:</b>	Switch Mode Power Supply
<b>IGBT:</b>	Insulated Gate Bipolar Transistor
<b>EMF:</b>	Electro Motive Force
<b>PCB:</b>	Printed Circuit Board
<b>MCU:</b>	Micro Controller Unit
<b>UART:</b>	Universal Asynchronous Receiver/Transmitter
<b>PWM:</b>	Pulse Width Modulation
<b>ADC:</b>	Analog to Digital Converter
<b>ZVS:</b>	Zero Voltage Switching
<b>ZCS:</b>	Zero Current Switching
<b>TTL:</b>	Transistor-transistor logic
<b>EMC:</b>	Electromagnetic Compatibility
<b>CE:</b>	Conducted Emission

## LIST OF TABLES

<b>Table 3.1:</b>	Cost down with Jitter.....	27
<b>Table 4.1:</b>	List of Equipments.....	30
<b>Table 4.2:</b>	Harmonic Limits for Class A equipment.....	39
<b>Table 4.3:</b>	Efficiency of Cooking Methods.....	40
<b>Table 4.4:</b>	Test Results for Efficiency .....	40

## LIST OF FIGURES

<b>Figure 1.1:</b>	Layers of an induction efficient pan	2
<b>Figure 1.2:</b>	Induction Cooker	2
<b>Figure 1.3:</b>	(a) Simplest form of a transformer (b) Secondary shorted transformer	3
<b>Figure 1.4:</b>	Current Density vs skin thickness graph	6
<b>Figure 1.5:</b>	Induction Cooker Block Diagram	7
<b>Figure 2.1:</b>	Switching Loss for Hard Switching	11
<b>Figure 2.2:</b>	Current vs Frequency during resonance	15
<b>Figure 2.3:</b>	Quasi Resonant Topology	17
<b>Figure 2.4:</b>	Equivalent Circuit of the Resonant tank	17
<b>Figure 2.5:</b>	Resonant tank during switching	18
<b>Figure 2.6:</b>	The intervals during switching	19
<b>Figure 2.7:</b>	Quasi Resonant Topology	21
<b>Figure 2.8:</b>	Half Bridge Topology	21
<b>Figure 3.1:</b>	The change in $V_{CE}$ level with respect to the on time	24
<b>Figure 3.2:</b>	The change in the $V_{CE}$ level in case Jitter Method is applied	25
<b>Figure 3.3:</b>	The $V_{CE}$ level and the CE first harmonic for different Jitter algorithms	25
<b>Figure 3.4:</b>	Cycle to cycle frequency change algorithm	26
<b>Figure 4.1:</b>	Experimental prototype	29
<b>Figure 4.2:</b>	Quasi Resonant Topology with parameters	30
<b>Figure 4.3:</b>	$V_{GE}$ , $V_{CE}$ , $I_{Lr}$ instantaneously	32
<b>Figure 4.4:</b>	$V_{GE}$ , $V_{CE}$ , $V_{micro}$ , $I_{IGBT}$ instantaneously	33
<b>Figure 4.5:</b>	$V_{GE}$ , $V_{Lr}$ , $I_{Lr}$ instantaneously	34
<b>Figure 4.6:</b>	$V_{GE}$ , $V_{Cr}$ , $I_{Cr}$ instantaneously	35
<b>Figure 4.7:</b>	$V_{GE}$ , $V_{CE}$ , $V_{DC}$ instantaneously	36
<b>Figure 4.8:</b>	$V_{in}$ , $I_{in}$ instantaneously	38
<b>Figure 4.9:</b>	Harmonics of the system	39
<b>Figure 4.10:</b>	Current Transformer in Quasi Resonant Topology	43
<b>Figure 4.11:</b>	Current trf. Primary current, the secondary voltage	44
<b>Figure 4.12:</b>	$V_{GE}$ , $V_{CE}$ , Pan signal in case there is a pan	45
<b>Figure 4.13:</b>	$V_{GE}$ , $V_{CE}$ , Pan signal in case there is an aluminum pan	47
<b>Figure 4.14:</b>	$V_{GE}$ , $V_{CE}$ , Pan signal, micro gate during operation	48

<b>Figure 4.15:</b> IGBT protection algorithm	48
<b>Figure 4.16:</b> The square wave for standby	50
<b>Figure 4.17:</b> Current Transformer voltage during Soft Start	51
<b>Figure 4.18:</b> $V_{ac}$ Data signal vs input voltage	52
<b>Figure 4.19:</b> 50 Hz signal vs input voltage	53

## LIST OF SYMBOLS

$i_x$ :	Current Density at distance x
$I_1$ :	Primary current
$I_2$ :	Secondary current
$Z_L$ :	Secondary Impedance
$I_S$ :	Switching Current
$V_S$ :	Switching Voltage
$P_S$ :	Switching Power Loss
$F_S$ :	Switching Frequency
$V_C$ :	Capacitor voltage in series resonant converter
$i_L$ :	Inductor current in series resonant converter
$E_C$ :	Capacitor energy in series resonant converter
$E_L$ :	Inductor energy in series resonant converter
$Z_0$ :	Characteristic Impedance at resonance
$\omega_0$ :	Resonant Frequency
$V_{dc}$ :	The voltage over the Bulk Capacitor
$L_R$ :	The inductance of the resonant Coil
$C_R$ :	The capacitance of the resonant Capacitor
$S_1$ :	The IGBT as the switch
$D_1$ :	The diode mounted reversely inside the IGBT
$V_{CE}$ :	The collector emitter voltage of the IGBT
$V_{GE}$ :	The gate emitter voltage of the IGBT
$I_{DC}$ :	The current through the bulk capacitor
$I_{Lr}$ :	The current through the coil
$I_{Cr}$ :	The current through the resonant capacitor
$V_{Lr}$ :	The voltage of the coil
$V_{Cr}$ :	The voltage of the resonant capacitor
$V_{ac}$ :	The rms value of the input supply voltage
$I_{IGBT}$ :	The Collector Emitter current of the IGBT

# CHAPTER I

## INTRODUCTION

### 1.1 Description of Induction Cooker

In order to describe an induction cooker, it is compulsory to start with the definition of electromagnetic induction and induction heating. The discovery of electromagnetic induction in 1831 by Michael Faraday led to the development of many types of induction heating applied systems. Electromagnetic induction refers to the phenomenon in which electric current is generated in a closed circuit by fluctuation of current in another circuit through a magnetic field. The very basic principle of induction heating is the fact that alternating current flowing through a circuit affects the magnetic movement of a secondary circuit located next to it. The discovery of Faraday as named electromagnetic induction led to the development of transformers, electric motors, and generators. However, in practice there were still some problems to be solved. Core loss that occurs during the process of electromagnetic induction was a crucial problem. This problem was tried to be minimized by laminating the magnetic frames. The lamination method minimizes the paths of eddy currents inside a core so that heating of the core is generally prevented.

Despite the measures described above, the heat loss that occurs during the process of electromagnetic induction was turned into productive heat energy in an electric heating system. The Industry has used this idea by implementing induction heating for welding, cooking, and melting. In these applications, induction heating has made it easier to set the heater parameters without the need of an additional external power source. Absence of any physical contact to heating devices prevents unintentional and unpleasant electrical accidents. High energy density is achieved by generating sufficient heat energy within a relatively short period of time.

The induction heating method is capable of functioning with all metals while induction cookers are designed to function only with ferromagnetic materials such as iron and steel that will allow an induced current to flow within them. Iron and its alloys respond best to

induction heating due to their ferromagnetic nature. Many companies produce special cookware for induction cooking. These pans are designed to absorb magnetic energy and spread the heat quickly and evenly resulting in higher efficiency and reduction of hot spots that can cause food to burn in some areas while still uncooked in others. For this purpose, special cookware includes basically three layers for efficient and even cooking. First layer and the third layer are made of stainless steel for maximum gain of induction heating. However, over the first and below the third layer, a layer of aluminum is applied inside the cookware. This layer provides even distribution of heat.

- 1) 18/10 stainless steel is non-reactive to food and easy to clean.
- 2,3,4) 1145 aluminum with a layer of 3004 aluminum between for even heat distribution.
- 5) 18/10 stainless steel for superior bond.
- 6) Magnetic stainless steel for efficient induction
- 7) 18/10 stainless steel resists pitting & rusting

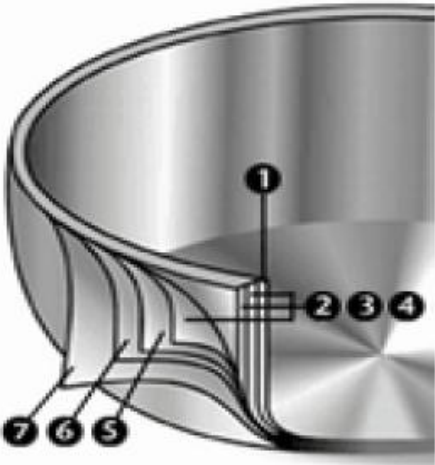


Figure 1.1 Layers of an induction efficient pan [1]

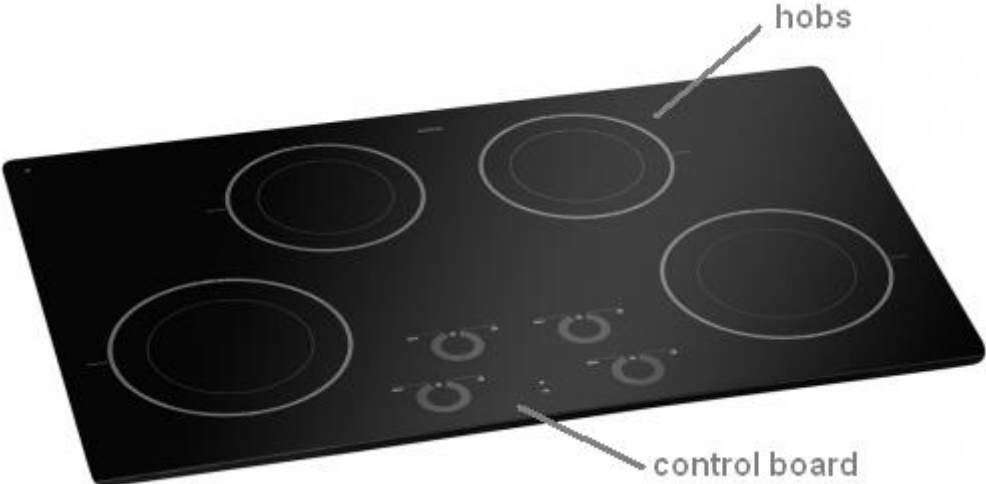


Figure 1.2 Top view of an induction cooker

As explained in [2], basic benefits of induction cooker compared to traditional gas or electrical cookers are efficiency, safety, speed, and controllability. Drawbacks include the fact that non-ferrous cookware such as copper, aluminum and glass cannot be used with an induction cooker. Additionally, the risk of accidental burning is diminished since the hob itself only gets marginally hot (due to heat conduction down from cookware) allowing direct contact with a reduced chance of accidental burning. Also, no heat is lost due to the air directly from the hob keeping the kitchen and cooker cooler. Once the pan is removed from the hob, the energy transfer stops. The result is a flameless method of cooking in which it is nearly impossible to start a fire by forgetting to turn off the cooker.

The control board of induction cookers, which generally include cap-sense (charge transfer as illustrated in [4]) method, can include additional functions such as Timer, Pause, Boost, Fry, Chocolate, Milk, Child Lock, etc.

**1.2 Basics Of Induction Heating**

**1.2.1 The Fundamental Theory**

There are three basic factors that affect induction heating. These are the electromagnetic induction, the skin effect, and heat transfer. However, the fundamental theory of induction heating is based on transformer theory. Figure 1.3 (a) illustrates the simplest form of a transformer, where the secondary current “ $I_s$ ” is directly proportional to the primary current “ $I_p$ ” according to the turns ratio  $N$  where  $N$  equals  $N_p/N_s$ . The primary and the secondary copper losses are generally caused by the resistance of windings.

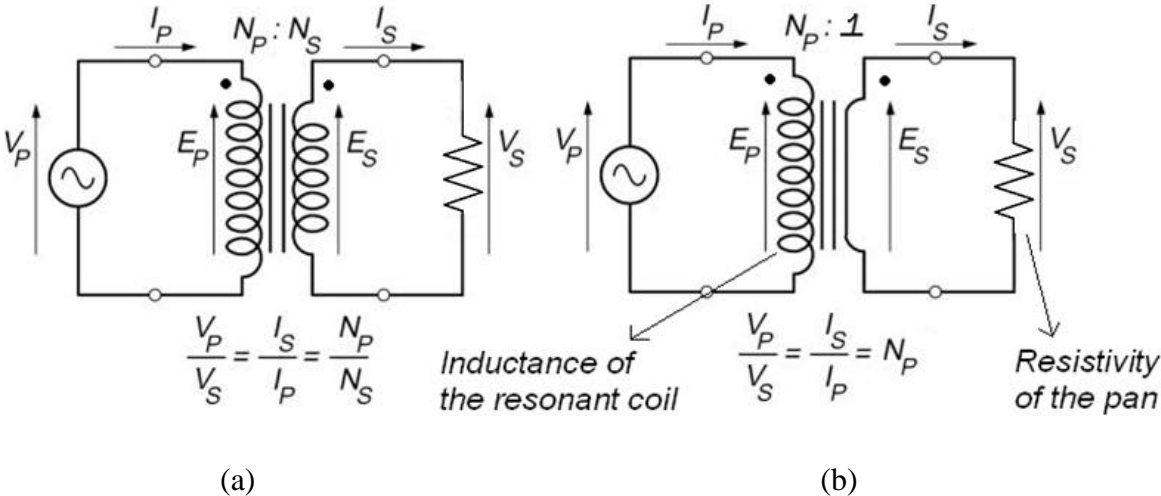


Figure 1.3 (a) Simplest form of a transformer (b) Secondary shorted transformer



When  $N_s$  is equal to one as the coil of the secondary circuit is turned only once, i.e. the secondary is short circuited, there is a highly increased heat loss due to the increased load current as depicted in Figure 1.3(b). This idea is the basic theory of induction heating.

The energy supplied from the power source is equal to the combined losses of primary and secondary ignoring other circuit losses. For safety reasons, the inductive heating coil and the load are insulated from each other by a ceramic glass with high insulation voltage as explained in [5].

As the main purpose of induction heating is to make the heat energy generated in the secondary maximum, the glass described above is designed to be as thin as possible while the secondary circuit, i.e., the pan in induction cooking, is made of a substance of low resistance and high permeability. Nonferrous metals decrease energy efficiency because of low permeability.

### 1.2.2 Electromagnetic Induction

When an alternating current with high frequency flows through a coil, a magnetic field is formed around the coil according to Ampere's Law.

$$\oint H dl = N i \quad (1.1)$$

In Equation 1.1,  $i$  is the coil current,  $dl$  is the integration path.

$$\Phi = \mu H A \quad (1.2)$$

In Equation 1.2,  $\Phi$  is the flux of the magnetic field through area.

The flux induces a voltage as shown in Equation 1.3 ( $E$ ) below the surface of the pan which produces the induced current as the secondary is short circuited. This induced current is called eddy current. The direction of the eddy currents are determined by the Lenz Law where the flux created by eddy currents is opposing to the original flux direction.

$$E = N \frac{d\Phi}{dt} \quad (1.3)$$

$$I = \frac{E}{R} \quad (1.4)$$

In Equation 1.3,  $E$  is the induced voltage. In Equation 1.4,  $I$  is the eddy current, and  $R$  is the resistivity of the secondary.

As a result, the electric energy caused by the eddy current is converted into heat energy as shown in the Equation 2.5.

$$P = E^2 / R = I^2 R \quad (1.5)$$

Magnitude of the current is determined by the intensity of magnetic field. Heat energy is inversely related to skin depth which will be described in the following section.

If the object mentioned has conductive properties like iron, additional energy of heat is generated due to the magnetic hysteresis. However, this additional energy loss is much smaller than the energy generated by eddy currents. Therefore, hysteresis losses are ignored.

### 1.2.3 The Skin Effect

The magnetic field produced by the coil generates induced current below the surface of the pan. This current circulates on the surface according to Lenz Law. As the working frequency of induction cookers is 20-30 kHz, the current on the surface is denser on the edges (skins) of the surface because of skin effect. The eddy current produces its own magnetic field. Since this magnetic field is in reverse direction with the flux, the current is denser on the edges. If the frequency of the current within the coil is higher, the induced current flowing around the surface of the load becomes more intensive. The density of the induced current decreases when flowing to the center as implied by the Equation 1.6 and 1.7. This phenomenon is called the skin effect. By this idea, it is obvious to state that the heat energy converted from electric energy is concentrated on the skin depth (surface of the object) as shown in [6].

$$i_x = i_0 e^{-x/\delta} \quad (1.6)$$

In Equation 1.6,  $i_x$  is the current density at distance  $x$  which is the distance from the skin of the object,  $i_0$  is the current density on the surface ( $x=0$ ), and  $\delta$  is a constant determined by the frequency (skin depth constant).

$$\delta = \sqrt{\frac{2\rho}{\mu\omega}} \quad (1.7)$$

In Equation 1.7,  $\rho$  is the resistivity of the pan surface (ohms meter),  $\mu$  is the permeability of the pan surface (henry/meter), and  $\omega = 2\pi f$  as  $f$  is the frequency of the current flowing through the pan surface (Hz).

Equation 1.6 clearly illustrates that the skin thickness is determined by the resistivity, permeability and the frequency of the applied current. Figure 1.4 is the distribution chart of current density in relation to skin thickness “x”. When x equals  $\delta$ , the current drops down to  $e^{-1}$  i.e. 36% of its initial value.

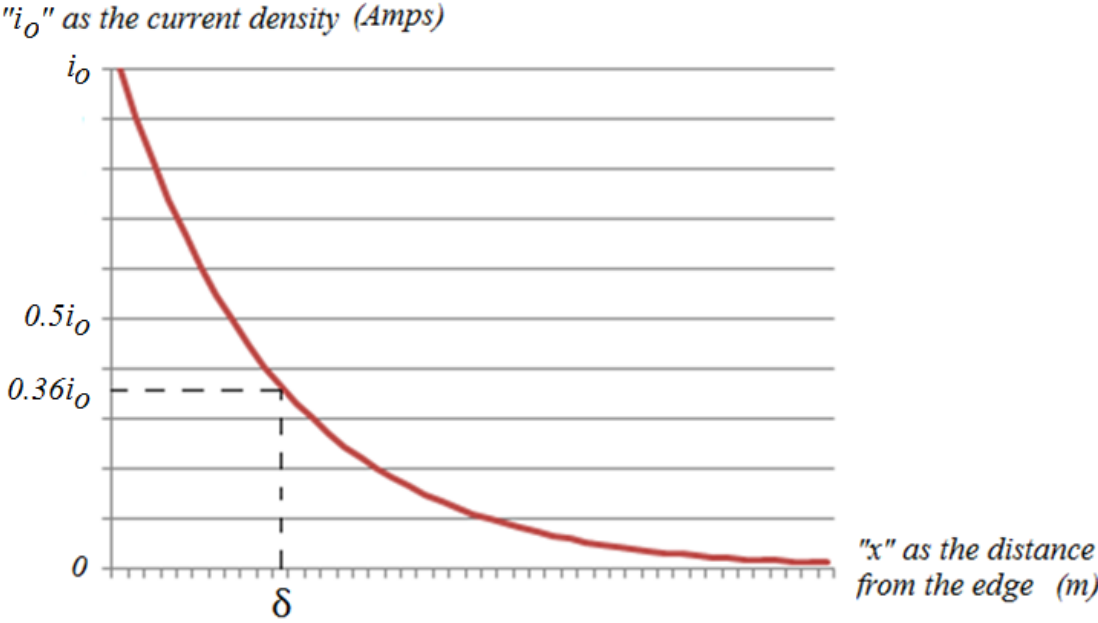


Figure 1.4 Current density vs skin thickness

**1.3 Induction Cooker System Features**

Figure 1.5 is the block diagram of an induction cooker. Multi output flyback topology is used for the SMPS. Auxiliary voltages are required for control issues. +15Vdc is especially necessary to drive the IGBT and the blower fan. However +5Vdc is required mainly for the microcontroller. The transformer used in SMPS is small in size due to the high frequency used to obtain the mentioned voltages. This helps to reduce the cost of the PCB. The relay is generally for safety purposes. When the microcontroller turns the hobs off; it also turns the relay off to ensure safe operation. The details for the quasi resonant topology will be explained in the next chapter. So in this chapter, the general system features are mentioned.

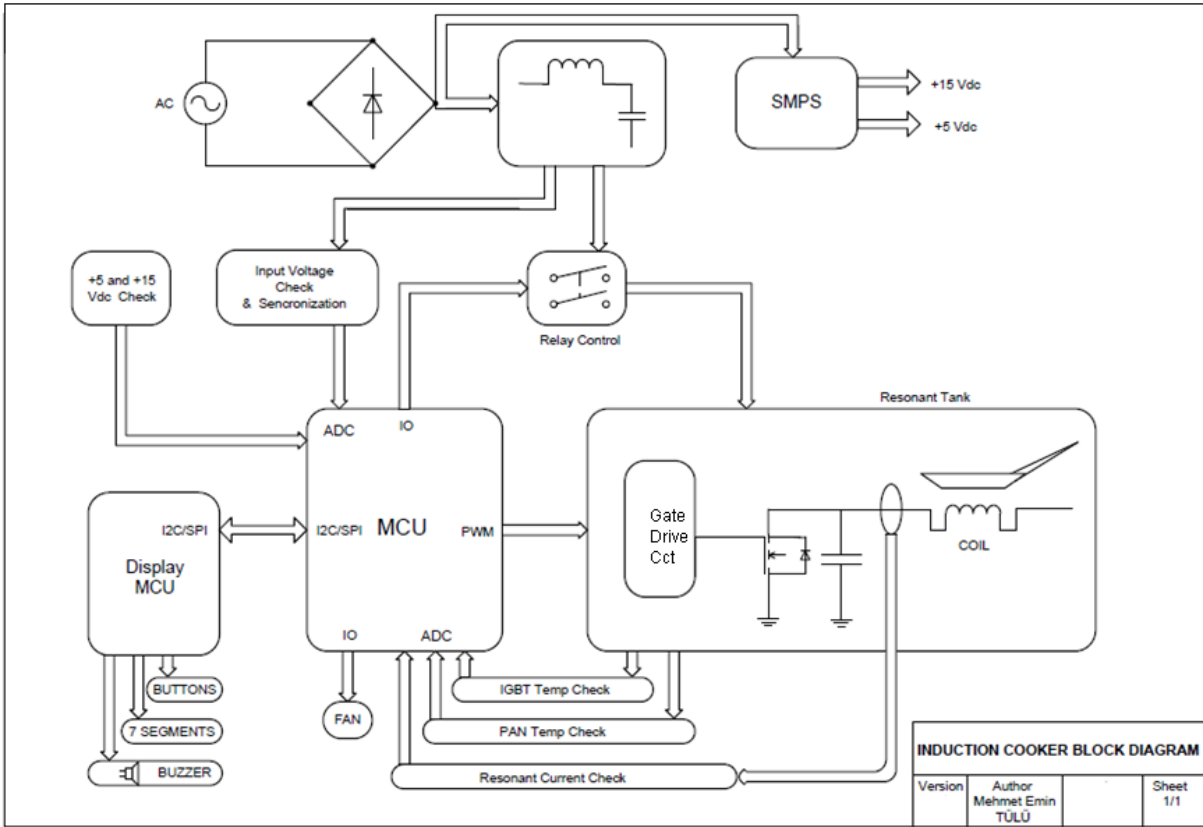


Figure 1.5 Induction cooker block diagram

There are four hobs (heating element) in Vestel induction cooker. One power board controls two hobs. So in one induction cooker, there are two power boards and a touch control board. The microcontroller in the touch control board acts like the Master while the other two MCUs in the power boards act like the slave. So the relationship between the Master and Slave is that the Master tells whether the Slave will work a hob or not. The Slave reports the Master if any kind of failure occurs in the system. So the Master decides the next operation. The communication is carried out through UARTs among the MCUs. The MCU in the touch control board also controls the buttons, seven segments, and the buzzer, where the touch control unit is capacitive.

The main job of the MCU in the power board is to drive the IGBT. The specifications of the IGBT are chosen according to the information in [7]. To drive the IGBT, the MCU applies a PWM signal whose on time and off time may change according to the data received by the MCU. For instance, if a less ferromagnetic pan is placed on the hob, the on time is increased by the MCU so that the same power can be transferred to that pan. Other than driving, the MCU also gets data from the sensors. These sensors are usually temperature and current sensors. There is one temperature sensor on each coil (hob) and also one sensor on the heat

sink where the IGBTs are mounted. The MCU applies different operations according to the data coming from these sensors. For instance, if the heat sink temperature increases, it works the fan, which may continue with the reduction of the heat level of the hob. Moreover, with some algorithm, whether the food in the pan is starting to burn or not can be determined via the temperature sensor in the coil as shown in [8]. If the rated utility voltage level of 220Vac increases, the MCU lowers the on-time in order to limit the power transferred to the pan. The synchronization with the frequency of the utility (50Hz mainly) is also necessary in many operations of the MCU. For instance, the MCU waits for the zero-cross of the utility voltage to turn off a hob to provide a less noisy turning off operation.

The resonant current value can be determined with a current transformer, details of which will be given in Chapter 6. The determination of the current level within the resonant tank through the IGBT or the Coil is necessary for many reasons. For instance, if the pan is removed slowly from the hob, the power transferred to the pan decreases automatically although the on-time is not decreased. When the power goes down, current through the resonant tank decreases, and the amount of reduction in the current is determined via the current transformer.

#### **1.4 Previous Work**

There are some studies conducted in the literature about frequency modulation (jittering) in induction cookers as in [22], [23], and [24]. However, these studies only point to the improvement in EMI problems. There is no referring to the IGBT voltage reduction or hindering mechanical vibration via Jitter Method. So, the contribution of the thesis to the literature can also be named as “Providing less IGBT voltage rating and hindering mechanical vibration noise via Jitter Method”. The frequency modulation algorithms in [22], [23], and [24] do not improve IGBT voltage rating as the proposed algorithms have no relation with the voltage after full wave rectification.

The closest method in the literature is [22]. The frequency is modulated to increase the EMI performance of the induction cooker. However, it has no improvement about the IGBT voltage rating reduction because the value of the frequency has no relation with the voltage after full wave rectification. The frequency is modulated in a triangular waveform (saw-tooth) but in a random timing as the two cases proposed in [22] have a jitter period of 6ms and 9ms. Moreover, the proposal in [22] is in half bridge topology while the thesis proposal is in quasi resonant topology.

[23] is also very similar to [22]. Different techniques are proposed to increase the EMI performance. However, [23] also does not provide any improvement for IGBT voltage rating reduction. Moreover, [22] or [23] do not refer to hindering the mechanical vibration noise at resonant frequency. The cost down with the application of Jitter Method is also not covered.

The application of frequency modulation method for power converters is shown in [24]. The method explained is used in many SMPS applications where the modulation is conducted by the switching IC which consists of a MOSFET mounted inside. This method also only points out to the improvement in EMI issues.

[25] proposes a new method of IGBT drive for Half Bridge topology. It is claimed that two dual outputs can be driven with this method. No improvement in EMI is referred in this paper.

The work in the literature about induction cooking has also been reviewed.

In [26], a modified ZVS flyback inverter with active clamp is covered. It proposes the use of an auxiliary switch in addition to the IGBT to decrease the voltage stress of the IGBT. It also uses an external resonant capacitor and an external resonant coil for this purpose. The method of changing the power output by changing the frequency is covered in [27] for Half Bridge topology. The analysis of the modes for IGBT drive has also been covered. The frequency is changed only to change the power output in [27] which is a basic implementation. Similar to [26], in [28] an external IGBT is used to provide soft switching for the main IGBT. The system is duty cycle controlled and basically there are 5 modes (intervals) for the IGBT drive in this type of application. The optimal manufacturing process for an induction cooker coil is proposed in [29]. The optimal positions for the ferrites under the coil are also shown. Temperature measurements over the coil are also conducted for different pan positions in [29]. [30] analyses the circuit operations under ZVS and NON-ZVS switching for Half Bridge topology. It also analyses the waveforms that appear if the phase angle is shifted. A new method in addition to quasi resonant topology and the half bridge topology is proposed in [31]. It is named as “new quasi resonant ZVS-PWM inverter with power factor correction”. In this method, an external IGBT is used in series to the main IGBT. The difference of this method to half bridge is that the series external IGBT is connected in reverse polarity with the main IGBT. It is claimed that the power factor correction is improved in this method. [32] is the basic quasi resonant topology analysis for an induction cooker system. The contribution may be that the optimum numerical values for the choice of the resonant coil and the

capacitor for different power outputs can be obtained in [32]. However, the power output values are too low in [32] as the range is 100-500W. In [33], the system is turned off for 2-3 ms when the input voltage reaches its peak. However, this type of application has no improvement for EMI problems. Also it is a noisy operation to turn on and off a system other than zero crossing instants.

## **1.5 Contributions of This Thesis**

The main contribution of this thesis is a new Jitter Method for an induction cooker application which reduces the IGBT Collector Emitter (CE) voltage rating while improving the conducted emission (EMI) problems and hinders the probability to drive a pan at its mechanical resonance frequency where the pan moves on the hob. The details of Jitter Method are explained in Chapter 3. As stated in the “Previous work” section, [22], [23], and [24] only address the EMI problems. By driving the coil at different frequencies, they actually also solve the vibration noise problem which is “not” mentioned in their papers. However, since the change in the frequency has no relation with the voltage after full wave rectification, IGBT voltage rating is not improved in [22], [23], or [24]. If the on-time of the IGBT is started to be decreased linearly from the zero crossing of the utility voltage for 5ms, and similarly increased after 5ms to the next zero crossing, the collector emitter voltage rating can be reduced. This method is shown as method III in chapter 3.

As a second contribution of this thesis, the quasi resonant topology and the related topics such as pan detection, delivered power detection, and the protection circuits were experimentally analyzed and tested. The results were revealed in detail and supported with figures. Moreover efficiency measurement has been conducted in Vestel Laboratories.

## CHAPTER II

### DESIGN AND ANALYSIS

#### 2.1 Theory

##### 2.1.1 Switching Action

There are two types of switching modes for transistors used in PWM applications. These are Hard Switching and Soft Switching as explained in [9]. If there is a resonant circuitry for switching and this circuitry is used to decrease the power loss, this is called soft switching. However, the power loss in Hard Switching is much higher than that of a soft switching application. In Hard Switching mode, a specific current is turned on and off at a nonzero voltage when the switching occurs. This loss is called as the Switching Loss. Increasing the frequency results in more switching in a period of time, and this leads to more switching loss in total. All types of switching cause an increase of the electromagnetic interference of the system because of a large amount of change in  $di/dt$  and  $dv/dt$  occurring in the process. Figure 2.1 illustrates voltage and current transitions during hard switching operation.

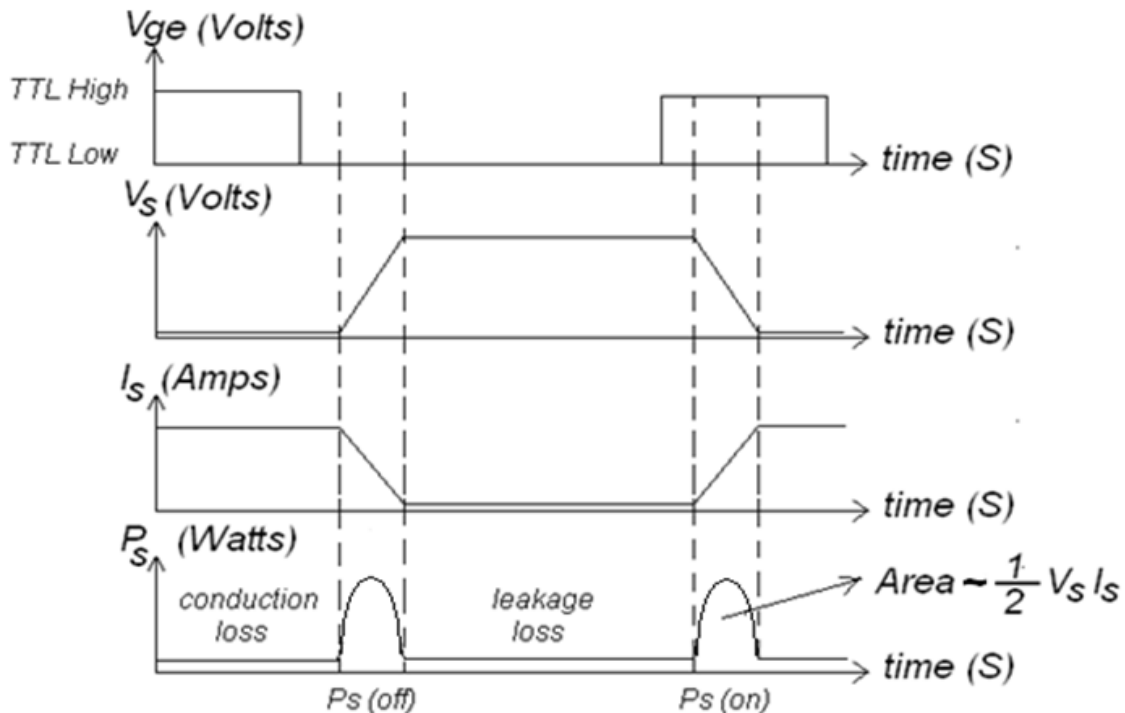


Figure 2.1 Switching Losses for Hard Switching



The total loss can be summarized as the sum of conduction loss, leakage loss, turn on loss, and the turn off loss for one period. Transistors have a forward voltage (for instance, for IGBTs the definition is referred as the collector emitter saturation voltage) which is nonzero and typically couple of volts. During conduction, this voltage multiplied with the conducting current ( $I_s$ ) gives the Conduction loss. Moreover, during blocking of the transistor, there is a leakage current through the transistor which also results in leakage loss if multiplied with the blocking voltage  $V_s$ . However, blocking loss is less considerable than conduction loss.

As shown in Figure 2.1, because of the structural behaviors of the transistors, when Gate is turned off or on, there is a delay time for the current/voltage to reach to the desired level. Also capacitors and inductors in the circuit hinder rapid changes in the voltage or current. These two issues construct the main reason for switching loss.

In the Figure 2.1, the area which corresponds to the multiplication of  $V_s$  and  $I_s$  during switching almost equals to the half of the total area. Then, since the total area equals  $V_s I_s$ , the loss can be indicated as  $\frac{1}{2} V_s I_s$ . Then;

$$P_s(on) = \frac{1}{2} V_s I_s \frac{t(on)}{T} = \frac{1}{2} V_s I_s f_s t(on) \quad (2.1)$$

Then total switching loss equals to;

$$P_s = \frac{1}{2} V_s I_s f_s ( t(on) + t(off) ) \quad (2.2)$$

In Equation 2.2 and Figure 2.1,  $P_s$  is the switching loss (Watts),  $V_s$  is the switching voltage (Volts),  $I_s$  is the switching current (Amps),  $f_s$  is the switching frequency (Hz),  $t(on)$  is the switching turn on time (seconds), and  $t(off)$  is the switching turn off time (seconds).

It is a known fact that increasing the switching frequency, the size of a transformer or a filter can be decreased. However, as explained above, higher frequencies result in low efficiency for the system. The switching loss causes the transistor get hot. There is a method that can avoid this situation. However, this method only hinders the loss to be in the transistor. The loss just shifts to some other circuitry. The method that is explained is the usage of Snubber Circuits. The current goes through the snubber circuit when the switch (usually a MOSFET) is off.

At high frequency switching, higher energy efficiency of conversion can be obtained by forcing the voltage or the current to become zero at the instant of switching. This method is

called “Soft Switching”. This method can be applied in two different ways: Zero Current Switching or Zero Voltage Switching. Zero Voltage Switching refers to the elimination of the turn on switching loss by having the voltage of the switching circuit set to zero just before the circuit is turned on. So, since the voltage becomes almost zero during switching, multiplication with current will not lead to any significant turn on power loss. Zero current switching is to avoid the turn off switching loss by allowing no current to flow through the semiconductor switch just before turning it off. Here, as the main concept of Soft Switching, the current or the voltage administered to the switching circuit can be made zero by the usage of the resonance created by the L-C resonant circuit. This topology is called a Resonant Converter.

As it will be also explained in the next chapter, the method used for induction cookers is Zero Voltage Switching, just like in many other different industrial applications. The voltage over the IGBT in OFF state almost reaches 1200 volts during switching for Vestel Induction cooker design. It is highly crucial to switch the IGBT to ON condition when this voltage reaches zero. Otherwise, the IGBT cannot withstand this amount of power loss during switching. In other words, it is not possible and reasonable to drive a quasi resonant topology circuit in Induction Cookers without the usage of ZVS or ZCS. Figure 2.5 is a typical ZVS application.

### 2.1.2 Resonant Converter

The resonant converters can be in two types: the series resonant converter and the parallel resonant converter as explained in [10]. These resonant converters consist of a capacitor, an inductor, and a load resistor. Moreover, detailed description of resonant converters and the method for the resonant frequency formulation can be found in [11].

To analyze the series resonant converter, first the energy of the inductor must be formulated. However, prior to that, we must define the current through the system.

$$i_L = i = \sqrt{2} I \sin(\omega t) \quad (2.3)$$

It is clear to see that the current of the inductor and the capacitor equals in series resonant converter. Then

$$i_L = i_C = i_R = i \quad (2.4)$$

Then the capacitor voltage is,

$$V_c = \frac{1}{C} \int i_c dt = \frac{1}{C} \int i dt = \frac{-\sqrt{2}I}{\omega C} \cos \omega t \quad (2.5)$$

The energy through the inductor and the capacitor can be derived as follows;  $i_c$

$$E_L = \frac{1}{2} L i^2 = L I^2 \sin^2 \omega t \quad (2.6)$$

$$E_C = \frac{1}{2} C v_c^2 = I^2 / \omega^2 C \cos^2 \omega t \quad (2.7)$$

As a sinusoidal voltage “ $v$ ” is applied to the circuit, electrical energy is stored in the inductor and then transferred to the capacitor. Resonance occurs when the capacitor and the inductor exchange energy between each other as illustrated in [12]. During resonance, the total energy stored in the system stays the same. However, in case of the existence of a load resistance  $R$ , the total energy stored goes down in each cycle of the resonance. The resonant frequency, which is also the speed of the energy exchange, is determined by the inductor ( $L$ ) and the capacitor ( $C$ ) as shown in Equation 2.9.

Then in order to determine the size of impedance  $|Z|$ , we sum the reactance of  $X_L$  and  $X_C$ , then put the load resistor into account. Then, we obtain,

$$|Z| = \sqrt{R^2 + (\omega L - \frac{1}{\omega C})^2} \quad (2.8)$$

At the resonant frequency, the reactance of the capacitor and the inductor individually equal to each other for minimum  $|Z|$ . In Equation 2.9, the resonant frequency is obtained. If the system is driven at the resonant frequency, i.e., the frequency of the power supply is equal to the resonant frequency, the maximum possible amount of current flows through the circuit. This current decreases if the supply frequency is decreased or increased. In the case of an induction cooker, the resonant capacitor and the inductor (coil) determine the resonant frequency. If the IGBT's are driven in a frequency close to the resonant frequency, the efficiency is increased and higher power can be transferred to the pan.

Then the resonant frequency is;

$$f_0 = \frac{1}{2\pi\sqrt{LC}} \quad (2.9)$$

The characteristic impedance is (that is the impedance at resonance);

$$Z_o = X_L = X_C = \omega_0 L = \frac{1}{\omega_0 C} \quad (2.10)$$

Then  $Z_o$  can also be written as  $\sqrt{\frac{L}{C}}$  by deriving from Equation 2.10.

In the presence of a load resistance  $R$ , another quantity called the quality factor  $Q$  is defined as;

$$Q = \frac{\omega_0 L}{R} = \frac{1}{\omega_0 C R} = \frac{Z_o}{R} \quad (2.11)$$

The value of  $Q$  is chosen to be smaller in induction cookers unlike RLC circuits or transformers as the heat losses are beneficial in induction cookers. In other words;  $Q = \omega_0 L / R = \omega_0 L i^2 / R i^2 = \text{produced} / \text{consumed energy}$ .

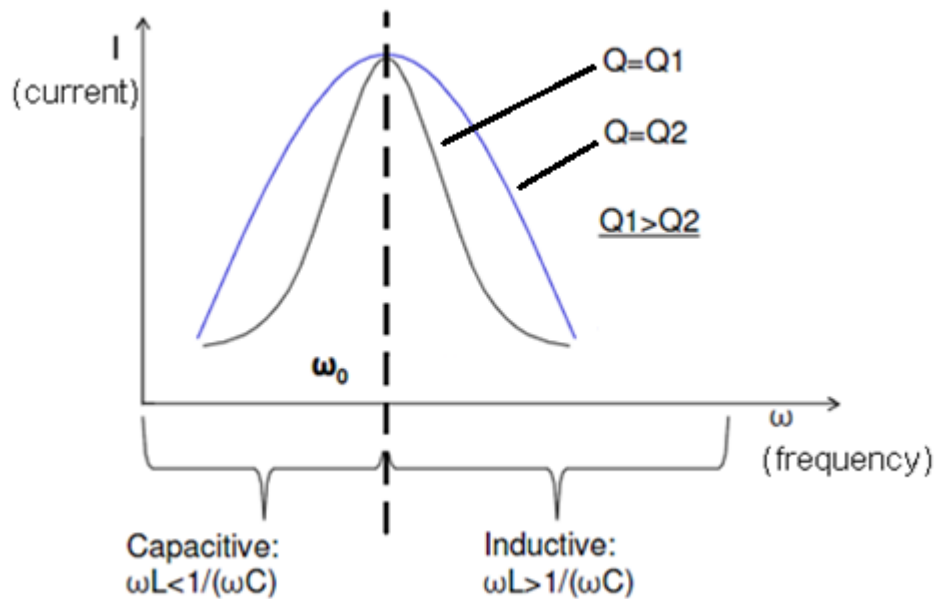


Figure 2.2 Current vs Frequency during resonance

As can be seen in Figure 2.2, if the system is driven at the resonant frequency, the maximum amount of current and the power can be obtained for quasi resonant or half bridge topology induction cooker. However, driving the induction cooker in exact resonant frequency causes

vibration and noise on the pan. That is why generally working frequencies close but not equal to resonance frequency is chosen for induction cooking.

Equation 2.11 and Figure 2.2 leads to many significant results about the issue. For instance, if the resistance is smaller than the inductance, we obtain a larger  $Q$  value as the working frequency gets closer to the resonance frequency.

For the capacitive region where the switching frequency is lower than the resonant frequency, the inductive reactance is directly proportional to switching frequency, i.e., if the inductive reactance increases, the switching frequency increases and the output current increases until the resonant frequency.

Likewise, in the inductive region, the switching frequency is higher than the resonance frequency. In this region, the inductive reactance is bigger than the capacitive reactance. In this region, a higher switching frequency increases the impedance  $Z$ . This results in the transfer of less power. On the other hand, if the frequency is decreased, the equivalent impedance is decreased and the power transferred is increased. It is a known fact that higher switching frequencies increases the heat loss of the IGBT's in the induction cookers, that is why higher working frequencies are generally not desired in terms of IGBT operation performance.

## **2.2 Quasi Resonant Topology (QRT)**

Before starting to QRT analysis in detail, it is helpful to remind the general operation theory of an induction cooker. The general operation theory of an induction cooker is as follows. First, the AC voltage coming from the power source is converted into DC form using a rectifier. Then, this DC voltage is connected to a high frequency switching circuit to provide high frequency current to the heating coil. In this case, according to Ampere's Law, a high frequency magnetic field is created around the heating coil. If a conductive object such as a pan is put inside this magnetic field, then an induced voltage and an eddy current is created on the pan surface. These eddy currents generate heat energy on the surface of the pan.

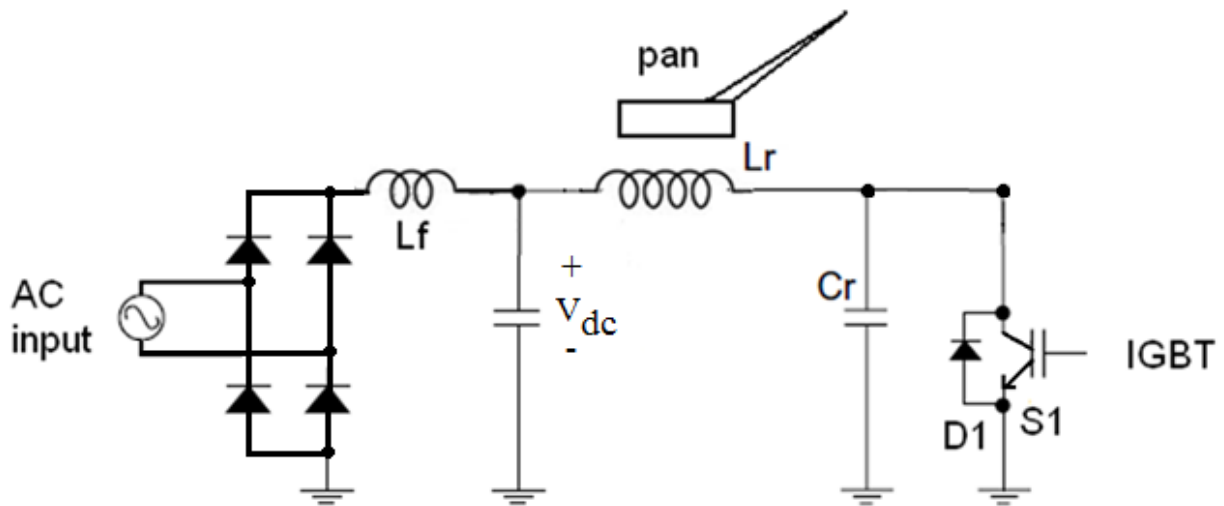


Figure 2.3 QRT

In Figure 2.3, the general concept of QRT induction cooker is illustrated. The capacitor that provides “ $V_{dc}$ ” voltage can be called as the bulk capacitor. However, the capacitor shown as “ $C_r$ ” in the circuit is called the resonant capacitor while “ $L_r$ ” is called as the resonant inductor or simply the “Coil”.

It is necessary to show the equivalent circuit of the resonant tank as in Figure 2.4.

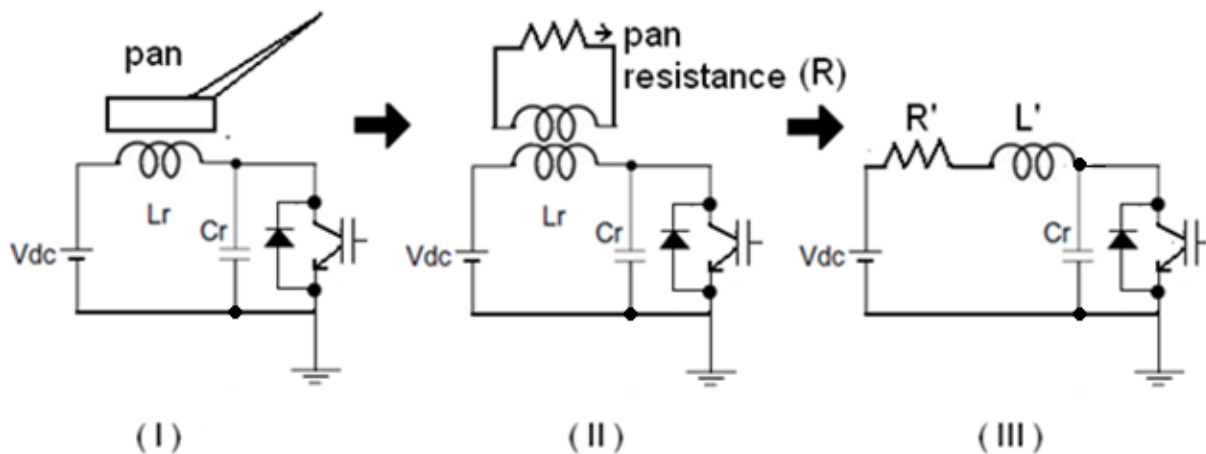


Figure 2.4 Equivalent circuit of the resonant tank

As seen in Figure 2.4, the system can be modeled as a transformer where the pan is modeled to be the secondary of the transformer. The pan is also modeled as a series combination of an inductor and a resistor as shown in (II). The reason is that the pan has permeability and resistivity. These two circuits can be modeled in a simpler form as in (III).  $R^*$  is the equivalent of the resistor in (II).  $L^*$  is the resonant inductor combination of  $L_r$  of the primary circuit, the leakage inductance and the secondary inductance.

The equivalent of the main resonant circuit is shown in Figure 2.4. Moreover, Figure 2.5 shows the waveforms of each block of the main resonant circuit in a cycle.

The system can be modeled in four intervals that fully cover the resonance occurring within the main resonant circuit. Below, the Interval 1 is chosen to be the beginning of the events and Interval 4 is chosen to be the ending of the events. In other words, the instant starting with the IGBTs ON to OFF mode is chosen to be the beginning interval.

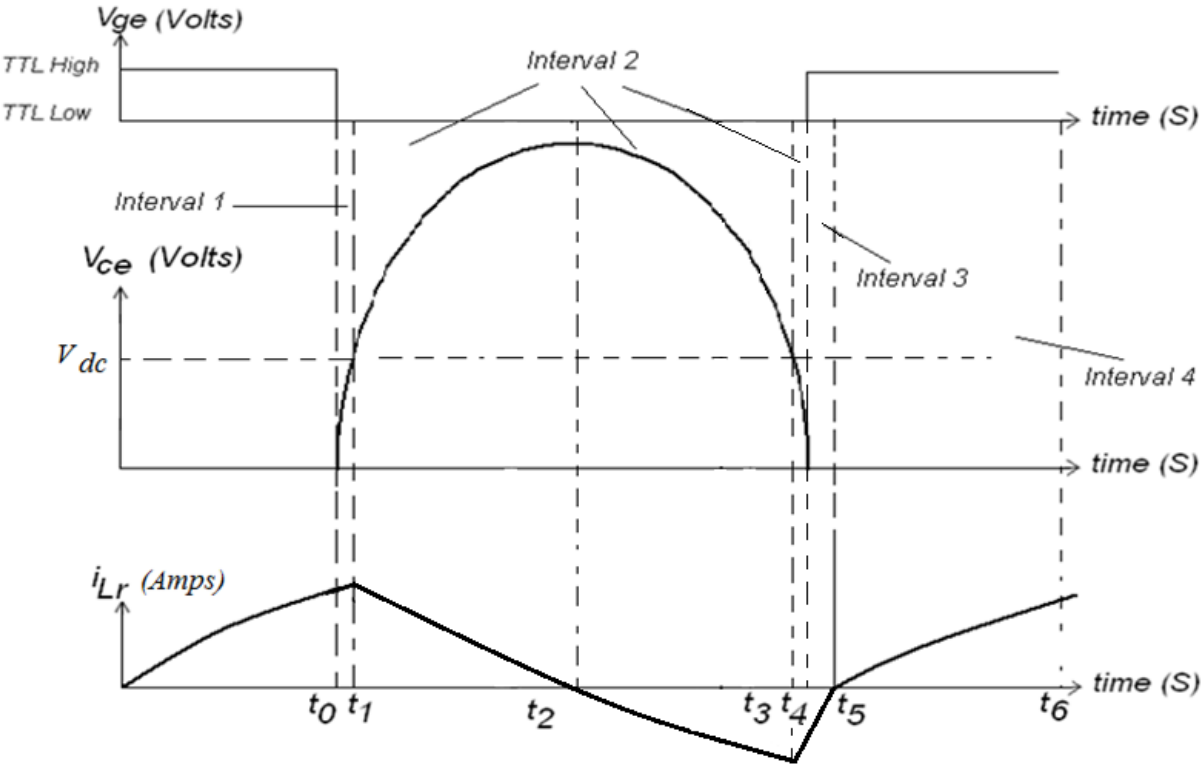
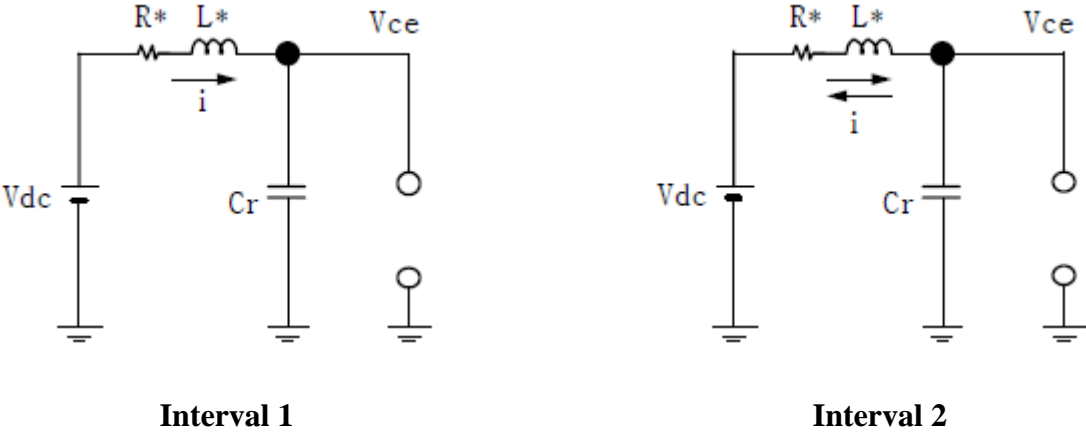


Figure 2.5 Resonant tank during switching



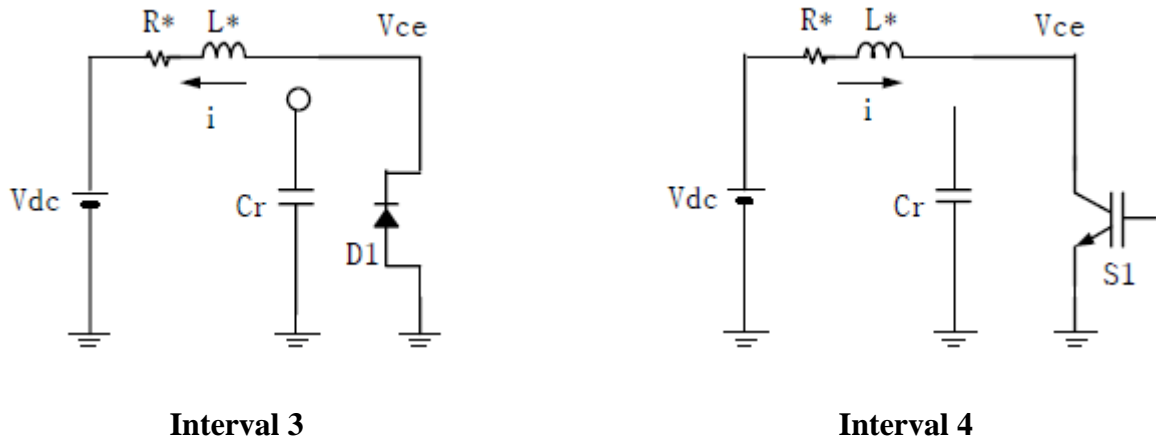


Figure 2.6 The intervals during switching [11]

### Interval 1, $t_0-t_1$

At  $t=t_0$ , the resonant current through the Coil or the IGBT is at its peak around 20-30 amperes. Turning off the IGBT at this instant causes turn off power loss. Since the current is coming from an inductor, it cannot end rapidly. The current starts charging the resonant capacitor and the charging interval is very little because of the high current between  $t_0$  and  $t_1$ . At  $t=t_1$ , the capacitor is charged to the same level as  $V_{dc}$  level. The  $V_{dc}$  level can be said to equal to  $220\sqrt{2} = 310$  volts. Actually, the current through the coil “ $i$ ” continues to increase until  $t=t_1$ . At the instant  $t_1$ , where  $V_{Cr}$  turns out to equal  $V_{dc}$ , the inductor starts to charge the capacitor.

### Interval 2, $t_1-t_4$

Since the inductor starts charging the resonant capacitor at  $t=t_1$ ,  $V_{Cr}$  becomes higher than  $V_{dc}$ . The current decreases down to zero at  $t=t_2$ . At this instant ( $t_2$ ), the resonant voltage over  $C_r$  reaches its maximum. This instant is also the instant where the inductor stops charging the capacitor and the capacitor starts charging the inductor instead. Then the current starts to flow in the opposite direction since  $V_{Cr} > V_{dc}$ . At  $t=t_3$ , the current is minimum as negative value. The voltage level of  $C_r$  had started to decrease at  $t=t_2$  and  $V_{Cr} = V_{dc}$  at  $t=t_3$ , which means the resonant capacitor voltage is again going to start to be lower than the voltage of the bulk capacitor. After  $t=t_3$ , the current again starts to increase as shown in Figure 2.6. The discharge is completed at  $t=t_4$  as  $V_{Cr} = 0$ .

### Interval 3, $t_4-t_5$

Although the voltage of  $C_r$  decreased to zero at  $t=t_4$ , the current is still flowing in negative direction because of the inductor effect, but the current is going to reverse direction at  $t=t_5$ .



The point here is that, now, since  $V_{Cr} = 0$ , the current must find a path for itself to complete the flow. The reason why the IGBT's have a diode in reverse direction mounted inside is this purpose.  $D_1$  is forward biased until  $t=t_5$ . Another very important detail in here is that the IGBT can be turned on before  $t_5$  as shown in Figure 2.6. However, since the current is still in reverse direction, the current flows through  $D_1$  not  $S_1$  until  $t=t_5$ .

#### **Interval 4, $t_5$ - $t_6$**

From interval  $t_5$  to  $t_6$ , the current flows through the IGBT. At  $t=t_6$ , the sequence turns back to Interval 1 as the IGBT is forced to turn off by the control circuitry. The IGBT must be turned on when the voltage across the IGBT is minimum to decrease the turn-on switching loss. In Vestel design of induction cooker, as it will be covered with more details in the following chapter, the instant when the voltage across the IGBT decreases to 0 is determined by an external circuitry. At this instant, the circuitry sends an interrupt to the microcontroller to turn on the IGBT. The MCU keeps the IGBT turned on according to the power needed. More on-time will lead to more power.

Note that the resonant capacitor  $C_r$  can be connected to the IGBT collector and ground. However, this capacitor can be connected totally parallel to the Coil as shown in Figure 4.1. In this case, the voltage that  $C_r$  must withstand is decreased considerably which helps to reduce cost and increase reliability. In this case, the current amount through the Coil does not change which means the same heating performance is still achieved. It must also be noted that the systems are generally driven above 20 kHz as this frequency is the limit for human hearing ability. Since very high frequencies cause switching loss to increase, frequencies between 20 and 30 kHz are chosen.

### **2.3 Half Bridge Topology and Comparison to QRT**

The widespread method for induction cookers is Half Bridge Topology. The reasons, advantages and drawbacks will be explained in this chapter. The QRT is mostly a new method to drive an induction cooker system. Before getting into details, it would be wise to go on with the figures of both methods first.

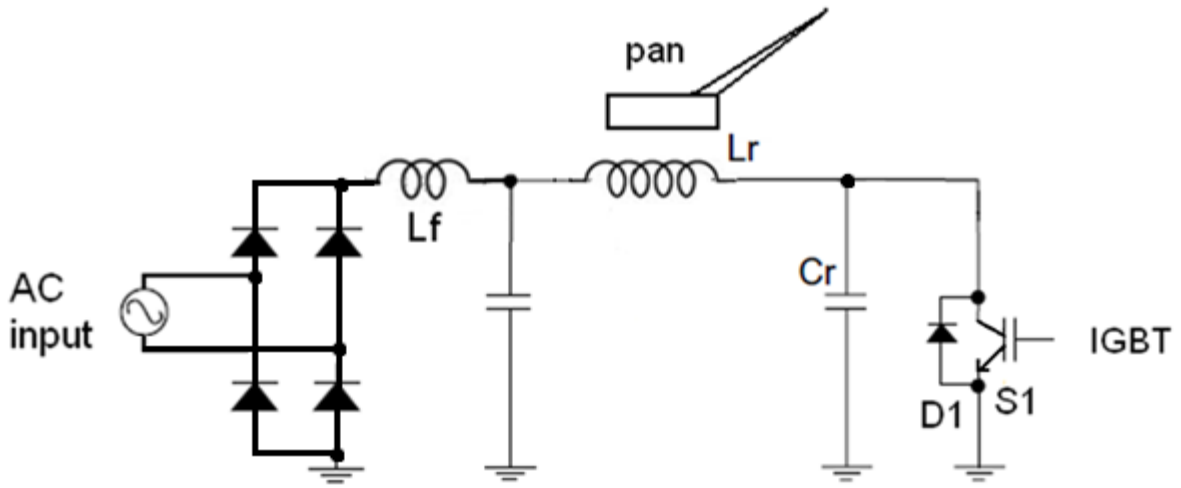


Figure 6.1 “QRT”

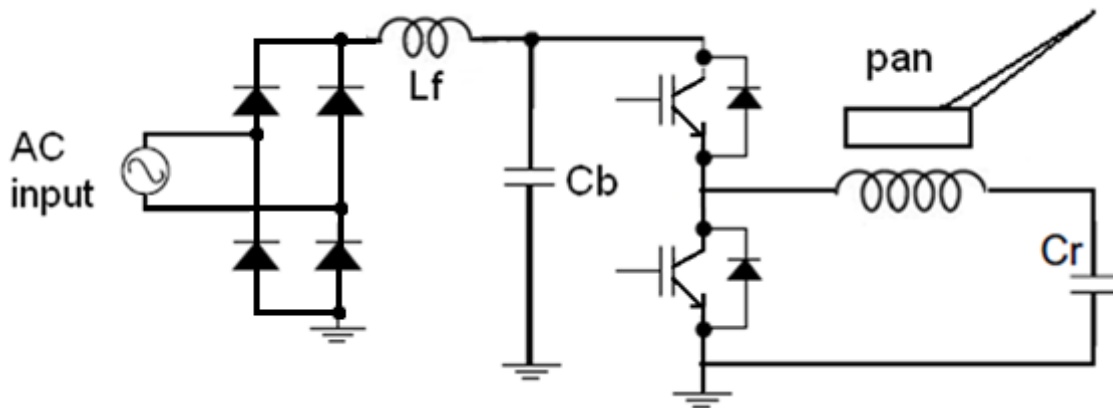


Figure 6.2 “Half Bridge Topology”

Till this chapter, the topology of quasi resonant has been explained. The topology of Half Bridge is similar to quasi resonant in basics. As explained in [17], in Half Bridge two IGBTs are used, which are activated one by one as High Side and Low Side. As the IGBTs are driven step by step, the current through the resonant tank reverses during resonance and similar results with QRT are obtained.

There are basically 4 intervals in the drive of half bridge topology. These are:

Interval 1: IGBT 1 ON IGBT 2 OFF

Interval 2: IGBT 1 OFF IGBT 2 OFF

Interval 3: IGBT 1 OFF IGBT 2 ON

Interval 4: IGBT 1 OFF IGBT 2 OFF

In Interval 1, the current through the coil accelerates and charges the resonant capacitor. In Interval 2, the accelerated current goes through the diode of IGBT 2 and decelerates. In Interval 3, IGBT 2 is turned ON as the current changes direction to pass through IGBT 2. In Interval 4, IGBT 2 is also turned OFF. The current finds a path over the diode of IGBT 1 this time. In all these Intervals, only in Interval 1, the resonant tank uses the energy of the bulk capacitor and the network.

Advantages of Half Bridge Converter Topology:

- The IGBT needs to withstand half of the voltage that it had to in QRT as explained in [1].
- Stable switching, more resistant to noise.
- The design of the switching control circuitry (High-Low side drive) is easy.
- The first EMC CE harmonic is stronger in Quasi resonant as there is a basic drive frequency around 25 KHz in that method as shown in [19].

Drawbacks of Half Bridge Converter Topology:

- Requires two IGBTs and switching circuitry, so “higher” cost.
- The heat sink and PCB size has to be bigger because of more IGBTs existence.
- More complex software as the actions must include both the IGBTs.

In Vestel design, the drawbacks have been solved by driving the system with jitter which made the QRT advantageous also with low cost. Also robust software and special grounding on the PCB contributed to the system. Note that the advantages of Half Bridge topology can be considered as the disadvantages of the QRT, vice versa.

## CHAPTER III

### JITTER METHOD

Jitter Method is to change the drive frequency with respect to the input voltage after full wave rectification. In other words, it is “not to” drive the system with an exact predetermined frequency but to drive it within a frequency range. In Jitter Method, the drive frequency is arranged for each 10ms (100Hz). One way of doing this is to increase the switching frequency between 3ms - 7ms and to decrease the frequency between 0ms - 3ms and 7ms - 10ms. By this arrangement, the power level can be kept the same. By this smart frequency arrangement, the three benefits shown below can be obtained.

- Less voltage rating for the IGBT
- Conducted Emission (EMC-CE) reduction
- No probability to drive a pan at its mechanical resonant frequency where the pan moves on the hob

The IGBT voltage reaches its peak at 5ms after zero crossing. If the frequency is decreased between 3ms-7ms, the IGBT voltage will reach a value which is less than its initial value. Moreover, if the system is driven with fixed frequency, there is a peak at the first harmonic around 25 kHz. Jitter Method removes the sharpness of the harmonic and makes it flat. In other words, it is possible to pass the CE test with less number of EMI filters on the electronic board. Lastly, driving a pan at electrical resonant frequency is not applicable as the pan starts moving on the hob and makes noise by vibration. In fixed frequency drives, it is possible to encounter a drive at resonant frequency for some old types of pans especially “enamel” types. Using Jitter Method clearly hinders this problem.

### Less voltage rating for the IGBT:

When the microcontroller is driving the system, the off time is constant, i.e., the off time interval cannot be changed by the MCU. The reason is that the resonance frequency of the system is affected only by the pan characteristic, the resonant coil, and the resonant capacitor. Moreover, even if the MCU tells the IGBT to turn on, the IGBT cannot turn on before zero crossing of the system. Then it is clear to state that the MCU can only adjust the on time of the IGBT. However, as the MCU changes the on time of the IGBT, the  $V_{CE}$  level changes. If the on time is increased, the  $V_{CE}$  level increases, vice versa. For instance, if the system is driven at 1500W,  $V_{CE}$  level reaches up to 800V. Nevertheless, if the system is driven at 2000W,  $V_{CE}$  level reaches up to 1000V. Since the IGBT is rated of 1200V, it is not reasonable to drive close to the peak voltage limit. As seen in Figure 3.1, if the on time is decreased from on time 1 to on time 2, the  $V_{CE}$  level also decreases from  $V_{CE1}$  to  $V_{CE2}$ . The reason is that less energy is stored in the resonant coil.

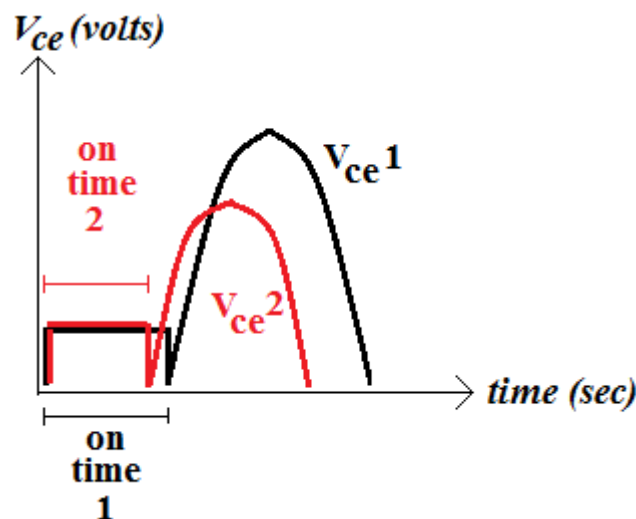


Figure 3.1 The change in  $V_{CE}$  level with respect to the on time.

It is clear that the  $V_{CE}$  level reaches its peak at 5ms after zero crossing. So it is wise to have less on time at these instants. Then, different algorithms can be applied to provide less voltage rating for the IGBT. Assume that the system is driven with 40 $\mu$ S (25kHz) and the on time is 20 $\mu$ S. Then it is a smart arrangement to increase the on time to 30 $\mu$ S for 0-2ms and 8-10ms after zero crossing, and to decrease the on time to 15 $\mu$ S for 2-8ms. Note that the increase and the decrease levels are not the same for different intervals. The reason is that less energy is provided to the resonant tank for 0-2ms and 8-10ms. In Figure 3.2, the change in the  $V_{CE}$  level in case Jitter Method is applied, is shown.

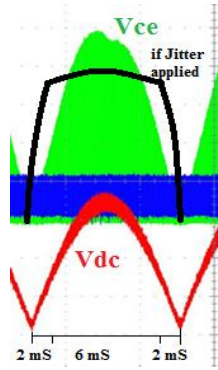


Figure 3.2 The change in the  $V_{CE}$  level in case Jitter Method is applied

Note that there are two frequencies in the example shown in Figure 3.2. The first one is in the interval 0-2ms and 8-10ms, and the second one is in the interval 2-8ms. However, as it will be explained in conducted emission reduction part, this type of jitter application results in still high conducted emission first harmonic as shown in Figure 3.3.

### Conducted Emission Reduction:

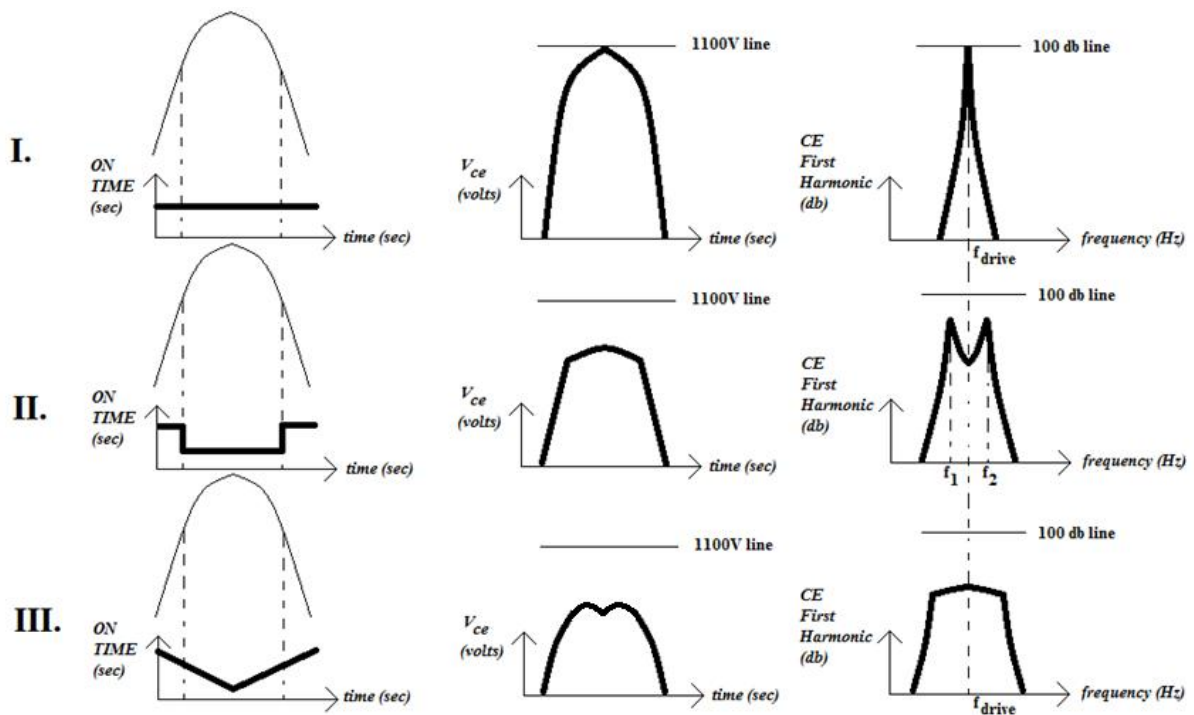


Figure 3.3 The change in the  $V_{CE}$  level and the CE first harmonic for different Jitter algorithms

As seen in Figure 3.3, different jitter algorithms with different on times result in different  $V_{CE}$  and CE first harmonic levels. If the on time is continuously decreased until 5ms after zero

crossing as in method III, the best result for conducted emission test and the least voltage over the IGBT can be obtained. Note that there are two drive frequencies at method II, which cause two peaks to appear in conducted emission test. Also note that the Jitter Method would not be necessary if the bulk capacitance was large enough to provide a voltage without considerable ripples.

One more algorithm (method IV) that can be applied as jitter is shown in Figure 3.4. This time the frequency is kept constant for a cycle (10ms) and changed in the second cycle. The problem with this type of application is that the  $V_{CE}$  level is increased. However, the EMC issues and vibration issues are still improved. The reason for the increase in  $V_{CE}$  level is that instead of “ $f$ ”, “ $f + \delta f$ ” and “ $f - \delta f$ ” is applied. For “ $f - \delta f$ ” case, the  $V_{CE}$  level increases.

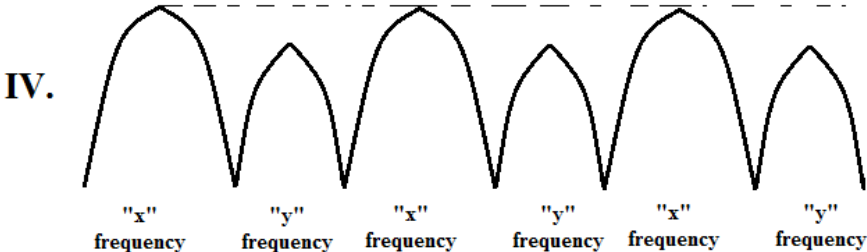


Figure 3.4 Cycle to cycle frequency change algorithm

Another algorithm would be to apply random frequency between a range (method V). This type of application would not improve IGBT voltage rating but still reduce EMC components. The saw-tooth method (method VI) explained in [25] can also be considered as method V, random frequency arrangement in terms of EMC improvement and IGBT voltage level. Since different frequencies are applied during operation, the EMC improvement is achieved. However, since the period is not determined to be exactly 10ms and the maximum frequency is not predetermined to be at 5ms after zero-crossing, no IGBT voltage improvement is achieved in [25]. The EMC improvements and IGBT voltage rating is similar in [25], [26], and [27].

Table 3.1 Cost down with Jitter

Method	# of EMC components removed	Removed EMC Component	Cost Down due to EMC improvement (\$)	Cost Down due to less IGBT voltage (\$)	Total Cost Down (\$)
I	0	-	0	0	0
II	1	X2 capacitor	1.2	0.3	1.5
III	2	X2 capacitor and line filter	2.8	0.4	3.2
IV	1	X2 capacitor	1.2	-0.3	0.9
V, VI as shown in [25], [26], [27]	1	X2 capacitor	1.2	0	1.2

Note that the total cost of the power board is around \$30. As shown in Table 3.1, some of the EMC components used in the power board can be removed for cost down for the same power output when Jitter Method is applied. Note that four different brand benchmarks were tested in Vestel laboratories and observed that they operate at fixed frequency (method I).

**Reduction of the vibration noise due to operation at resonance:**

As stated in chapter 2, the closer the drive frequency to the resonance frequency, the more power output is obtained. So, the system is designed to operate close to the resonant frequency. Note that the drive frequency changes when the MCU changes the working level of the hob. So, for some different types of pans and at various levels (8, 9, Boost, etc.), it is possible that the pan is driven at exact resonance frequency. In that case, the resonant tank delivers the maximum power to the pan which causes the pan to start moving on the hob due to high energy transfer. Moreover, in this case vibration occurs and the result is a noisy operation with a safety problem. Fixed frequency drives always have the possibility to encounter this problem. Since Jitter Method proposes to drive the system with different frequencies, this problem is automatically solved. For method II and IV, even if one of the two drive frequencies is the resonant frequency, the vibration noise decreases considerably relative to method I. The best result for mechanical vibration noise can be obtained with



method III, method V (random) or method VI (saw-tooth) applications as in [25], [26] and [27] since the drive frequency can only once be equal to the resonant frequency during the time interval of 10ms. Note that the audible noise could not be measured numerically due to the lack of the required equipments.

## CHAPTER IV

### EXPERIMENTAL RESULTS

#### 4.1 Results for QRT

Till this chapter, the theoretical results were analyzed. To check the consistency of the theoretical analysis to practical results, a power board with a power rating of 2300W was assembled. This power board consists of QRT as in Figure 4.1 for induction cooker system. Below can be seen the component values used to set up the QRT. About the choice of the resonant capacitor and the coil, the fact that the resonance frequency is between 20 kHz and 30 kHz is aimed. As explained in the previous chapter, over 30 kHz produces so much heat loss over IGBT and below 20 kHz makes the noise to be heard by human ears as explained in [13]. That is why a range between these two frequencies is provided via the choice of the resonant capacitor and the inductor.

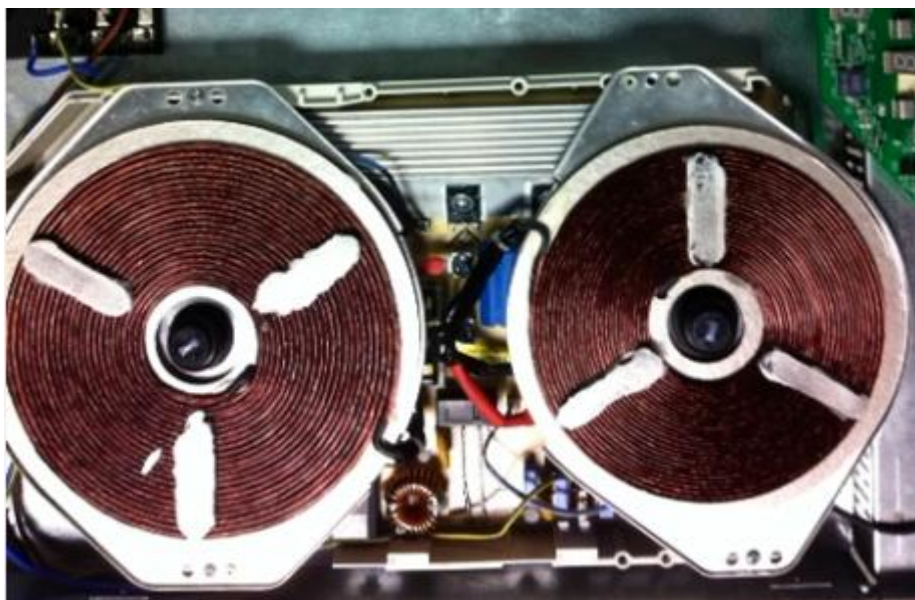


Figure 4.1 Experimental prototype

In Figure 4.1, the coils, the power board and the control board is displayed. As depicted in Chapter 1, one power board drives two hobs, i.e., two coils. The coil on the left side in Figure 4.1 has a diameter of 20cm while the smaller coil is 16cm. The 20cm coil has 28 turns. It is Class H rated as the temperature of the coil may go up to 150°C.

As explained in the previous chapter, the ground of the resonant capacitor can be connected to the positive node of the bulk capacitor ( $V_{dc}$ ) to provide the fact that the resonant capacitor needs to stand less voltage during the time when the IGBT is in OFF condition.

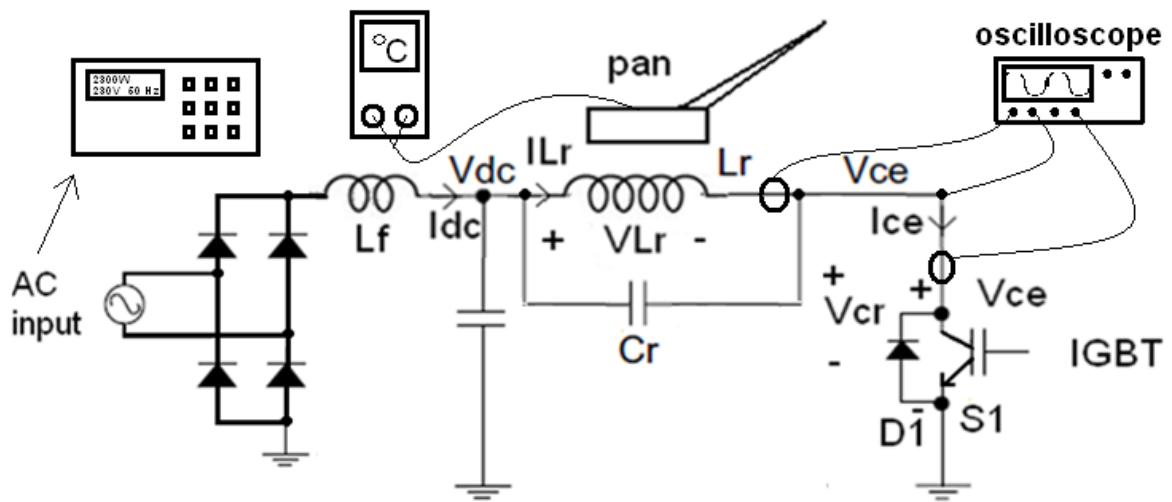


Figure 4.2 QRT with parameters

Table 4.1 List of Equipments

Type	Specifications
Oscilloscope	4 channels 1 GHz
High Voltage Differential Probe	4400V Max
Programmable AC power source	300V, 4000W Max
AC/DC Current Probe	50A, 20 MHz Max
Multi-meter	K type thermocouple used

In Table 4.1, the equipments that were used to obtain the experimental results are shown. During the explanation of the practical results,  $V_{coil}$  will stand for  $V_{Lr}$ ,  $I_{coil}$  for  $I_{Lr}$ ,  $V_{IGBT}$  for  $V_{ce}$ ,  $I_{IGBT}$  for  $I_{ce}$ ,  $V_{rescap}$  for  $V_{cr}$ , and  $I_{rescap}$  for  $I_{cr}$ .

A power board was assembled in the laboratories of Vestel to see the signals of the topology. When the input power is 1850W, the rms value of the current through the IGBT is 7.5A and

the peak current of the IGBT 19A for this configuration. Also the voltage of the IGBT reaches up to 1000 volts for this configuration (The voltage level which the IGBT must withstand is shown in [14]). These values must be within the acceptable range of the IGBT to provide reliable switching. The coil inductance is 80 $\mu$ H and the resonant capacitor value is 360nF for this configuration. The IGBT is rated of 1200V peak and 20A rms as maximum levels.

About the choice of the bulk capacitor of  $V_{dc}$ , Equation 4.1 is used. The Equation is the basic ripple voltage calculator for a full wave rectifier [21].

$$\Delta V = \frac{I_{dc}}{2 f C_b} \quad (4.1)$$

In Equation 4.1,  $\Delta V$  is peak to peak ripple voltage,  $I_{dc}$  is current of the inductor  $L_f$ ,  $f$  is the utility frequency, and  $C_b$  is the bulk capacitor.

The ripple value ( $\Delta V$ ) is important for pan detection which occurs before driving the system with high currents i.e. 8-10A. The system delivers around 0.07A before working a hob. The value of the ripple must not exceed 20% before pan detection. Now again calculating, as  $\Delta V=320 \times 0.2=64V$  we obtain,  $C_b$  equals minimum 10 $\mu$ F. That is why 10 $\mu$ F is chosen as the bulk capacitor. The system delivers around 10A with 50Hz. Calculating  $\Delta V$  for this case gives a huge ripple value. Figure 4.7 illustrates that when driving 10A, the effect of the bulk cap is negligible.

If Figure 4.3 is checked, it is seen that the system is driven with a period of around 42 $\mu$ S (23.8 kHz) with a power level of 1830W. Then in order to check if the system is driven below or over the resonant frequency, a simple calculation must be made with  $L_r$  (80 $\mu$ H) and  $C_r$  (360nF). As shown in chapter 4; the resonant frequency is;

$$f_0 = \frac{1}{2\pi\sqrt{L_r C_r}} \quad (4.2)$$

Then calculation gives us a resonant frequency of 29.6 kHz with this configuration. Then it is also obvious that the system is driven in capacitive region.

Note that as depicted in Figure 2.4, the value of inductance in Equation 4.2 differs with respect to the pan characteristic. For instance if the coil itself is 80 $\mu$ H, the inductance measured decreases to almost 60 $\mu$ H in case a highly ferromagnetic pan is placed over the coil. It is 70 $\mu$ H if an aluminum pan is placed. **Then it is clear to state that the resonant**

frequency differs with respect to the pan characteristic. The change is generally within 5-6 kHz range.

Different brand IGBTs like ST, Infineon, Toshiba, Renesas, Fairchild and so forth provide different characteristics during switching. These characteristics mostly appear as heat loss during switching. For instance, if the IGBT has high turn on-turn off times, the IGBT produces more heat during switching. That is why, to check the overall performance of the IGBT, it is a simple and quite consistent method to measure the temperature of the IGBT during a predetermined period of time. After comparisons, the best IGBT can be chosen.

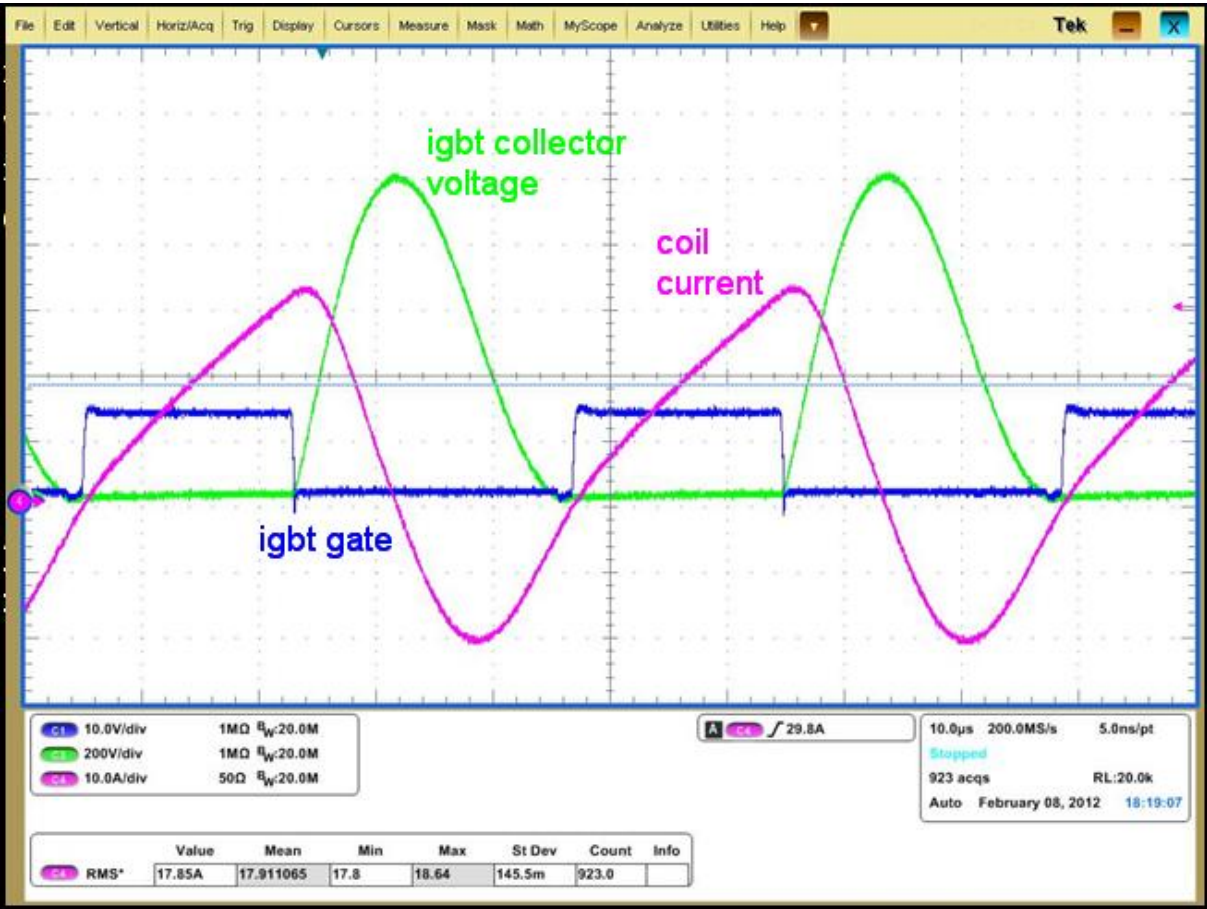


Figure 4.3 Coil current ( $I_{Lr}$ ) 10A/div, IGBT collector voltage ( $V_{CE}$ ) 200V/div, IGBT gate voltage ( $V_{GE}$ ) 10V/div, Time 10 $\mu$ S/div

Figure 4.3 is the experimental result (scope visual) of the QRT explained in **Figure 2.5 in Chapter 2**. If compared carefully, the signals are the same as the ones explained theoretically. The instant when the IGBT collector voltage drops down to zero during resonance, is determined via an external circuitry. At this instant the microcontroller turns the IGBT to ON condition to provide zero voltage switching. As the IGBT is ON now, the IGBT

collector voltage stays at zero value. Moreover, the current of the coil keeps increasing until the IGBT is again turned to OFF condition. This current starts to charge the resonant capacitor so starts to decrease. The detailed analysis of Figure 4.3 can be found in Chapter 2.

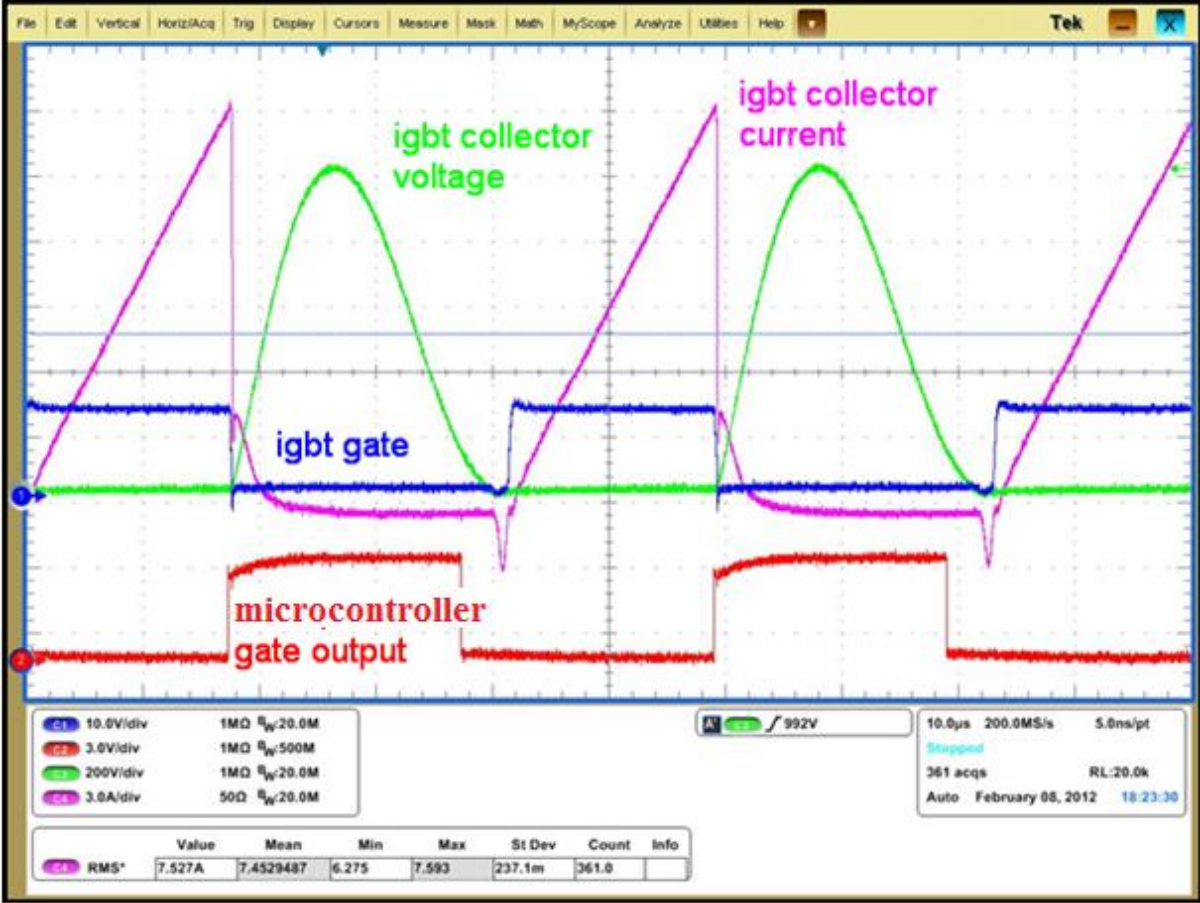


Figure 4.4 IGBT collector voltage ( $V_{CE}$ ) 200V/div, IGBT collector current ( $I_{IGBT}$ ) 3A/div,  
 IGBT gate voltage ( $V_{GE}$ ) 10V/div, Time 10μS/div,  
 Microcontroller gate voltage ( $V_{micro.}$ ) 3V/div,

As seen in Figure 4.4, the microcontroller gate output range of 5V is level shifted to the IGBT gate range of 12V using an emitter follower. The reason is that the IGBT is driven with 12V. The 5V is converted to 12V range by small signal BJT transistors. Also as seen in Figure 4.3, although the microcontroller tells the IGBT to turn ON, the IGBT waits for the voltage over itself to decrease down to zero to provide zero voltage switching. This is provided by an external circuitry. Moreover, again as seen in Figure 4.4, the microcontroller output and the IGBT gate is in reverse polarity i.e. when the microcontroller output is TTL Low, the IGBT gate is TTL High (ON).

The instant when “negative polarity” current passes through the IGBT is when the diode mounted inside the IGBT is in ON condition. This diode is in ON condition if the IGBT collector voltage is negative. It is clearly seen that the current of the IGBT starts to increase tremendously when the IGBT turns to ON condition. When the IGBT is turned OFF, all the current starts to charge the resonant capacitor. This means that the IGBT current drops radically to zero. However again as seen in Figure 4.4, there is still some current through the IGBT with positive value for a limited time when the IGBT is in OFF condition. The reason lies upon semiconductor nature so that if it is turned to OFF condition, some current still flows for a limited time. One other issue to be mentioned is that if the pan used is much less ferromagnetic, the power transferred to the pan can decrease considerably. For instance if the standard pan is driven with 2500Watts, the power delivered to an aluminum mixed pan can decrease down to 1000Watts with the same IGBT ON – OFF time when no other component values are changed. The efficiency of the system in this case stays the same. When the output power is decreased, the input power is also decreased. So this is not an efficiency issue.

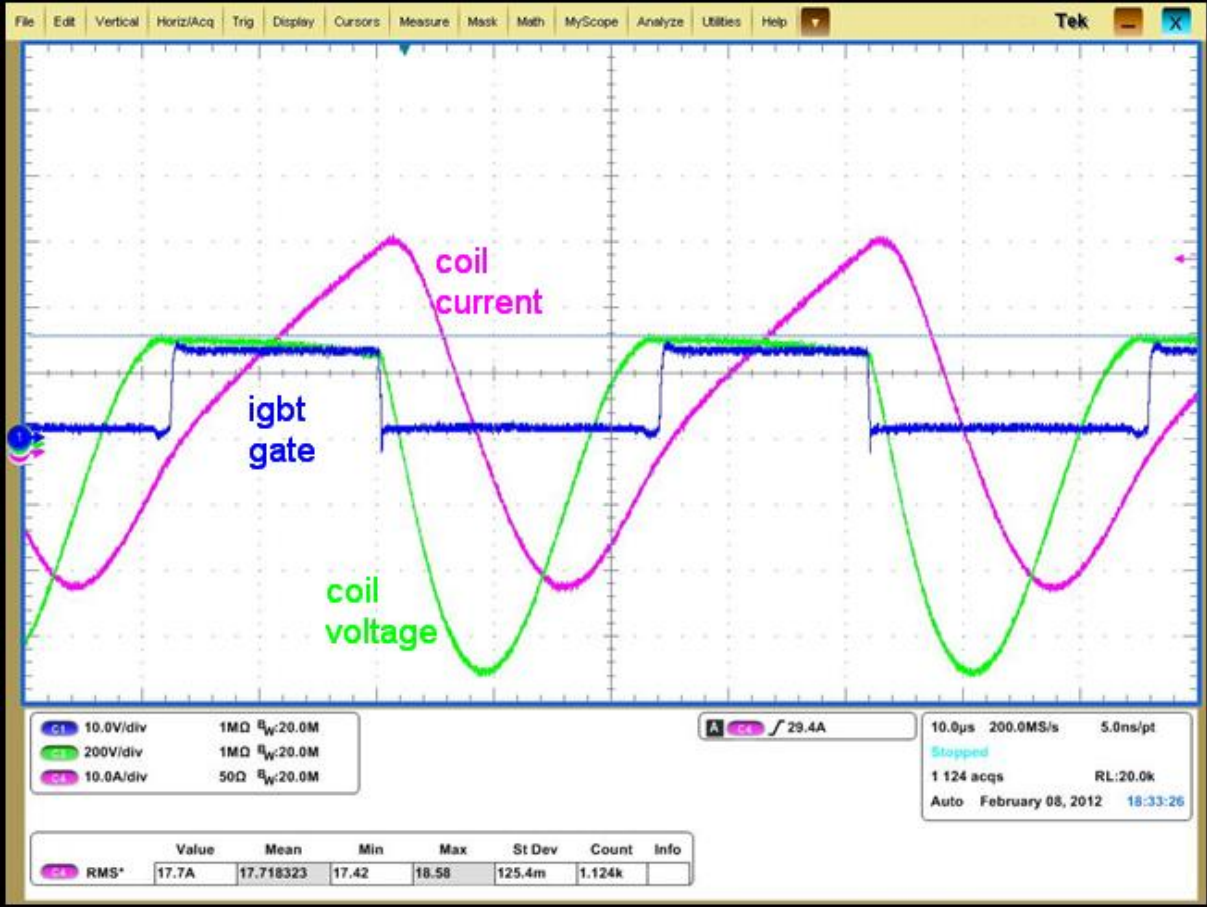


Figure 4.5 Coil voltage ( $V_{Lr}$ ) 200V/div, Coil current ( $I_{Lr}$ ) 10A/div, IGBT gate voltage ( $V_{GE}$ ) 10V/div, Time 10 $\mu$ S/div

When the IGBT is turned ON, the current through the IGBT starts increasing. This current is provided by the coil (inductor). In Figure 4.5, the coil current and voltage during different instants are shown.

As it is basic Power Electronics information, if the voltage of a coil is constant with a positive value during a period of time, the current through the coil keeps increasing with a constant rate. In Figure 4.5 the practical results are observed.

Note that when the IGBT is ON, the voltage over the coil is  $+V_{dc}$ .

Also note that when the IGBT is OFF, since the voltage of the coil is always the reverse of the voltage of the resonant capacitor, the shape of the voltage is decreasing to highly negative values.

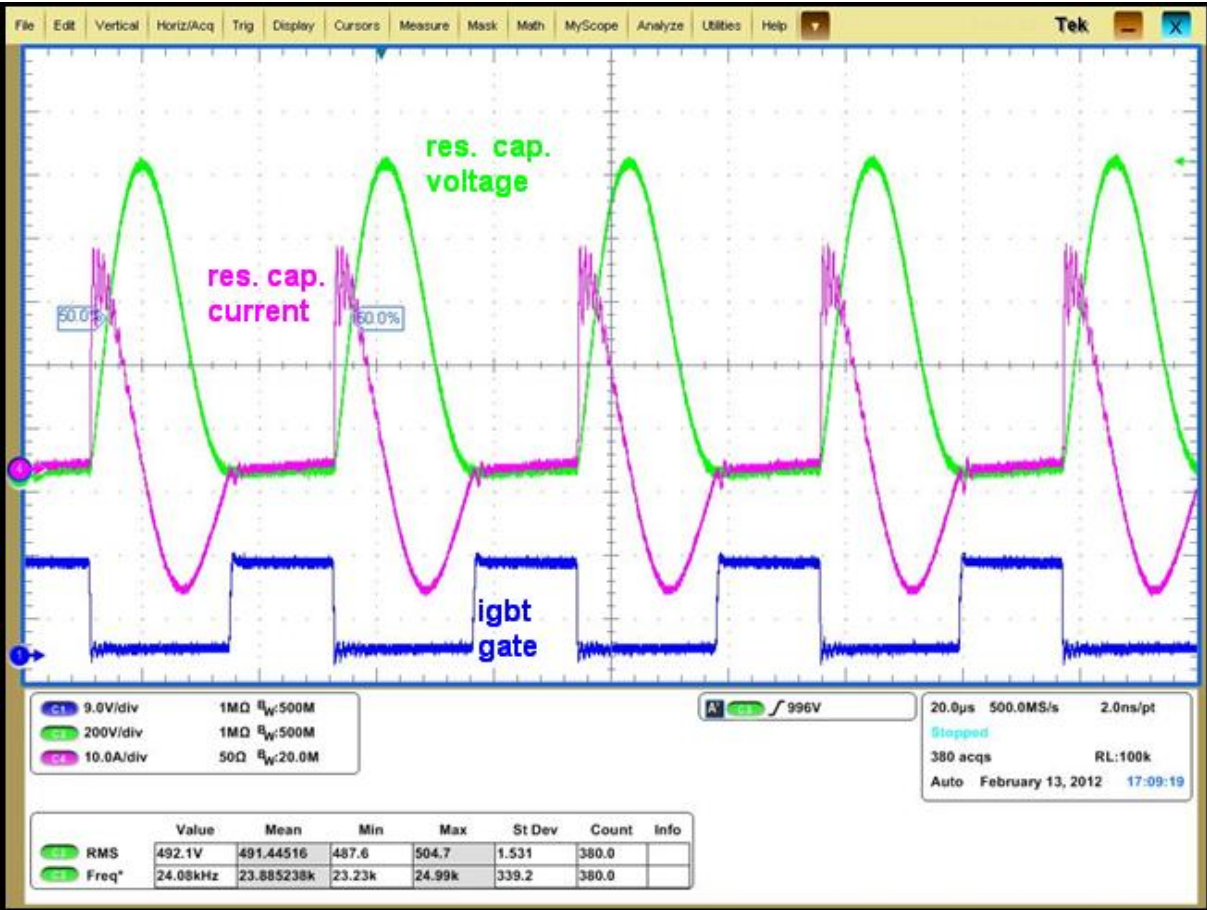


Figure 4.6 Res. Cap. voltage ( $V_{Cr}$ ) 200V/div, Res. Cap. current ( $I_{Cr}$ ) 10A/div, IGBT gate voltage ( $V_{GE}$ ) 9V/div, Time  $20\mu\text{s}/\text{div}$

As seen in Figure 4.6, when the IGBT is Turned ON, the voltage of the resonant capacitor is  $-V_{dc}$  volts which is around - 325 volts dc. However when the IGBT is turned off, the resonant



capacitor immediately starts to be charged by the resonant coil which provides a highly positive voltage value to the capacitor. But due to resonance, this voltage starts decreasing at a value where the resonant frequency determines.

Likewise, the current through the resonant capacitor gets a very positive value at the instant when the IGBT is turned OFF. The reason is that a very high current was flowing through the IGBT just before turn OFF. This current must continue from another path because of inductive characteristic of the coil. As the capacitor is charged, the current through it decreases as shown.

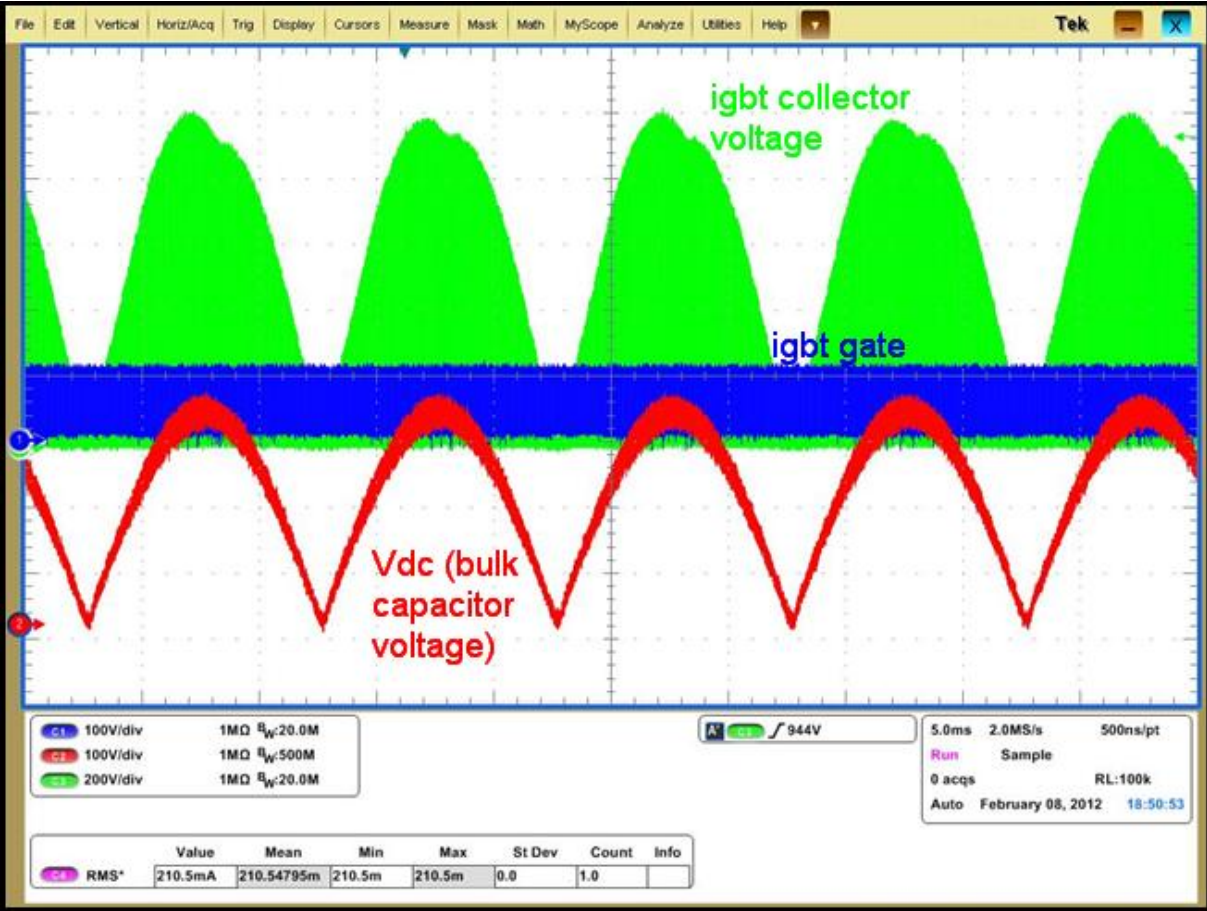


Figure 4.7 IGBT collector voltage ( $V_{CE}$ ) 200V/div, Bulk Cap. voltage ( $V_{DC}$ ) 100V/div, IGBT gate voltage ( $V_{GE}$ ) 10V/div, Time **5mS/div**

If the “Time Division” of the system is increased from 10uS to 5mS, we observe the signals as shown. It is clearly seen that the  $V_{dc}$  voltage which is supposed to stay at 325volts dc with some ripple voltage cannot stay at that level. The reason is that the output needs high power.

The high power driven by the system takes the energy of the bulk capacitor. The bulk capacitor discharges just in the shape of the signal provided to it by the rectifier. If the IGBT is turned off totally, the shape of the bulk capacitor voltage returns back to 325 volts dc level with some ripples.

As seen in Figure 4.7, at the instants where  $V_{dc}$  drops down to zero, the IGBT collector voltage also decreases to zero. The reason is that there is no energy that can be taken from the bulk capacitor. No current can flow the coil when the IGBT is ON. Then no voltage can be charged upon the resonant capacitor. These issues result in no collector voltage over the IGBT at those instants.

Note that the resonant frequency is the frequency where maximum power is transferred to the pan. However, every material also has a different mechanical resonance frequency that maximum electron movements are observed within that frequency. At that mechanical frequency, with the same amount of power consumption, more heating can be achieved. For instance by changing resonant capacitors or the resonant coils, assume that an aluminum particle is heated via induction at 30 kHz and 200 kHz. The system is arranged so that both conditions are the resonant frequencies. However, the mechanical resonance frequency is around 200 KHz for aluminum. Then, we can conclude that the temperature of the aluminum will be higher in case of 200 kHz drive frequency. In other words, driving at 200 kHz increases efficiency.

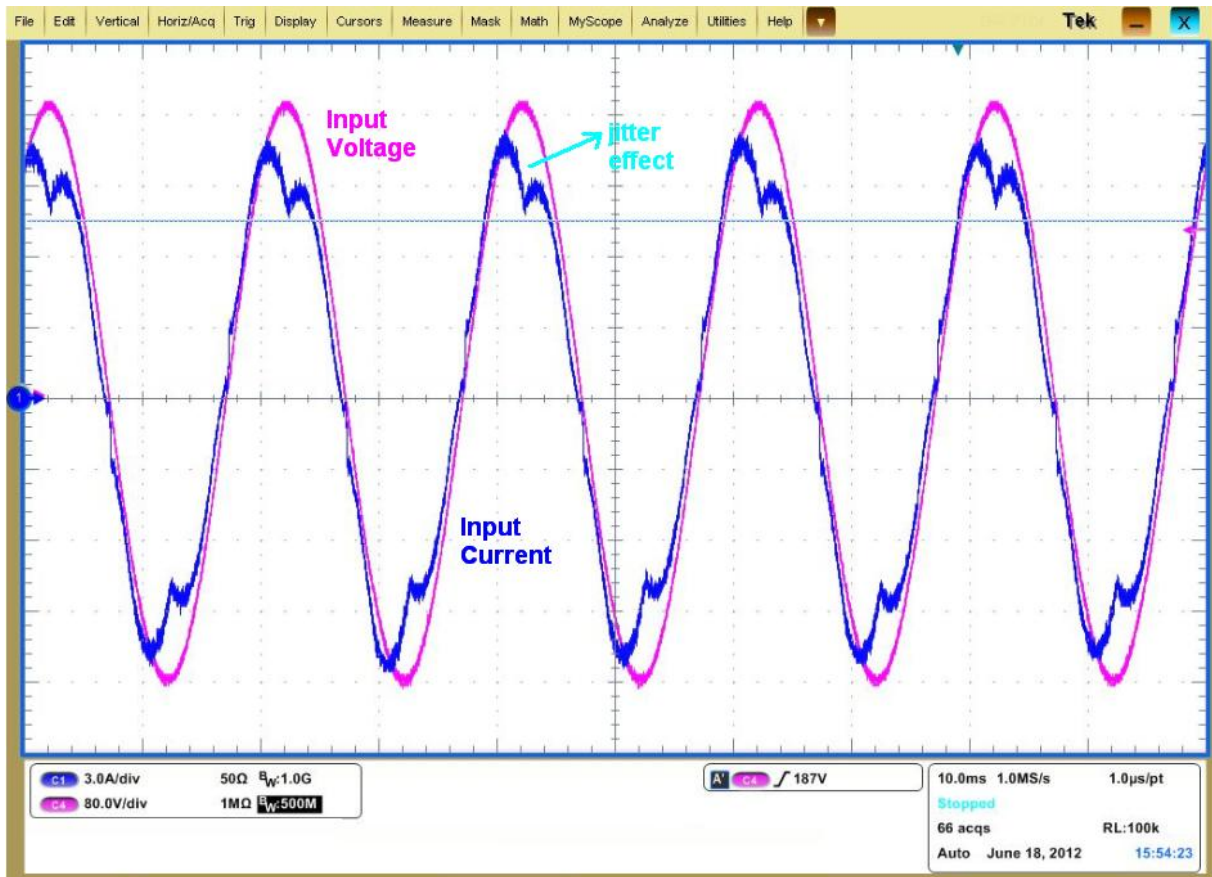


Figure 4.8 Input Voltage ( $V_{in}$ ) 80V/div, Input Current ( $I_{in}$ ) 3A/div,  
Time 10ms/div

The real power of the induction system in Figure 4.8 is 2030 Watts, the reactive power is 360 Var and the complex power is 2060 VA. The RMS of the input current shown is 8.95 A while the RMS of the input voltage is 230V. Then multiplication gives a value of 2060 VA as the complex power ( $PF = 0.983$ ). The system also consists of an EMI filter before the rectifier circuitry.

The harmonics of the system shown in Figure 4.2 was analyzed via a harmonics analyzer and drawn as shown in Figure 4.9.

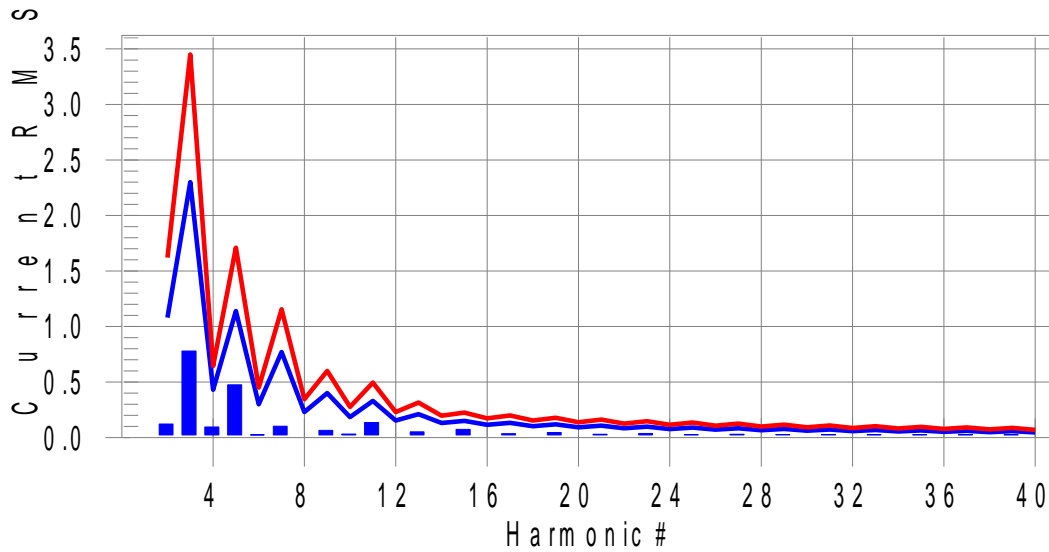


Figure 4.9 Harmonics of the system

The red line is the limit for the peak values that appear for every measurement conducted in one minute. The blue line is the limit for the average value of the measurements. As seen in Figure 4.9, the measurements – shown as bars - are within limits of TS EN 61000-3-2. Table 4.2 shows the numerical values of the limits for Class A equipment. Induction cooker is Class A equipment since it is a household appliance.

Table 4.2 Harmonic Limits for Class A equipment [20]

Harmonic order n	Maximum permissible harmonic current A
<b>Odd harmonics</b>	
3	2,30
5	1,14
7	0,77
9	0,40
11	0,33
13	0,21
$15 \leq n \leq 39$	$0,15 \frac{15}{n}$
<b>Even harmonics</b>	
2	1,08
4	0,43
6	0,30
$8 \leq n \leq 40$	$0,23 \frac{8}{n}$

## 4.2 Efficiency Measurement and Uncertainty Analysis

As stated in chapter 1.1, the efficiency of induction cooker is very high since the bottom surface of the pan is heated directly. According to the statistics taken from [3], the efficiency is highest in induction cooker as shown in Table 4.3.

Table 4.3 Efficiency of Cooking Methods [3]

Cooking Method	Efficiency
Induction	90%
Halogen	58%
Electric	47%
Gas	40%

Table 4.3 also clearly gives an indication about cooking time. The tests done in Vestel Laboratory confirms the result given in Table 1.1 in terms of speed. Using the same amount of electrical energy, two liters of water can be boiled almost two times faster than an electric or gas cookers. However, the tests conducted in Vestel laboratories reveal that the efficiency of induction cooker is around 82%. The efficiency also differs with respect to the brand of the induction cooker. To test the efficiency, 2kgs of water ( $c = 1\text{cal/gr}^\circ\text{C}$ ) is heated from  $25^\circ\text{C}$  to  $100^\circ\text{C}$ . Then the heat required is obtained as  $150000\text{cal} = 627000\text{joules} = 174\text{Wh}$ . Table 1.2 is the measurement result for efficiency of different types and brands of cookers. Note that Vestel Electric is a cooker with “resistive heating”.

Table 4.4 Test Results for Efficiency

Brand	Type	Input Power (kW)	Cooking Period (sec)	Input Energy (Wh)	Output Energy (Wh)	Efficiency
Vestel	Kettle	1.75	385	187	174	93%
Midea	Induction	1.68	461	215	174	80%
Sauter	Induction	1.79	444	221	174	78%
Dixions	Induction	1.75	429	208	174	83%
Ego	Induction	1.75	422	205	174	84%
Vestel	Induction	1.80	421	211	174	82%
Vestel	Electric	1.55	852	367	174	47%

Uncertainty analysis is required as the measured values for induction cookers are different than declared in [3]. There are two values measured during the test in Table 1.2 which are the temperature and the input power. Note that the equipments that were used to obtain the results in Table 1.2 are shown in Table 4.1. The multi-meter that measures the temperature via thermocouples shows no decimals for temperature. This means that the multi-meter measures in increments of 1°C. So the system uncertainty is 0.5°C. However, since there are two (final and initial) temperature measurements, the system uncertainty for this case is  $0.5^{\circ}\text{C} \times 2 = 1^{\circ}\text{C}$ . Moreover, putting into account the multi-meter device error of 1% according to datasheet (range from -40°C to 400°C) which makes around 4.4°C for this case, the total uncertainty is 4.13°C. Then, calculating the required output power for 69.6°C and 80.4°C gives us 161.5Wh and 186.6Wh respectively. Putting the 0.02% (200 ppm) device error of the energy meter also into account (range 4000Wh), the 211Wh value can be minimum 210.2Wh; maximum 211.8Wh. For worst case calculation,  $161.5/211.8=76,2\%$  minimum and  $186.6/210.2=88.7\%$  maximum is obtained. Then, to obtain the uncertainty in efficiency, 76,2 is subtracted from 88.7 and the result is divided by two, providing an uncertainty of 6.2. So, for Vestel Induction cooker,  $82.5 \pm 6\%$  is the efficiency containing the uncertainty of the digital multi-meter and the energy meter.

### **4.3 Control and Protection Issues**

Induction cooker system needs to be closed loop controlled. The reason is to provide reliability and quality for customers. In this chapter, the control and protection issues are covered.

#### **4.3.1 Delivered Power Detection**

It is a very significant issue to determine the power delivered to the pan. During normal operation of the cooker, the voltage of the network can be considered to be constant (230Vac). Because of this reason, we may also call this issue “Delivered Current Detection”.

There are several reasons why the delivered current needs to be known by the microcontroller as explained in [6]. First of all, there are levels in an induction cooker. These are Level 8(1600W), level 9 (2100W), and Level Boost (2500W), etc. Considering the voltage constant, it is a predetermined issue how much “current” a level will require. Then we can calculate that level 9 must deliver  $2100/230=9,1\text{A}$ . The microcontroller has the duty to provide this much

current to the system in all conditions (except input voltage changes.) The microcontroller knows how much current is flowing with the help of the delivered power detection system.

Secondly, in case a less ferromagnetic pan is placed on the cooker (assume aluminum mixture); if there was no system of delivered power detection, the power delivered to the pan would decrease considerably, even half of the ferromagnetic pan case as explained in [15]. Here, the microcontroller would use the same ON and OFF times for the IGBTs' so less power would be transferred. However, with the help of the delivered power detection system, as the microcontroller realizes that less current is flowing through the system, the microcontroller increases the ON time so that the power delivered is again increased. The microcontroller aims to provide the same current (power) to all types of pans. It achieves this by adjusting the ON and OFF times. Nevertheless, in the software there is also a maximum and minimum limit for the ON time. So finally, if a less ferromagnetic (aluminum) pan is placed, the microcontroller starts to work with the maximum ON time. It may not be able to provide the exactly the same current to the system because of the maximum ON time limitation but still the power delivered is only 100-200 Watts under the target value. If there was no system of delivered power detection, the power would be maybe 1000Watts under the target value which is 2500W for Boost Level.

Thirdly, one other benefit of this system is to provide similar powers to smaller pans. If a 16cm diameter pan is placed instead of a 25cm one, the system again tries to provide as much power as it can to reach the same current value as it is the target.

So again the ON time is increased by the microcontroller. Similarly, there are pans whose bottom base is much "more" ferromagnetic than assumed. Especially some old types of pans (especially "enamel" type), would try to acquire maybe 3500Watts instead of 2500 Watts. This also can not be allowed by the microcontroller. The microcontroller decreases the ON time in this case.

Lastly, since the components used have tolerances on the electronic board, the real power driven from the system and the power driven which the microcontroller knows must be "calibrated". In other words, the microcontroller may know that 1600Watts is provided to the system but it may actually be 1700Watts. Especially the tolerance of the "delivered power detection system" may cause this power difference. So in the production line of Vestel, a power meter tool and the microcontroller of the electronic board communicates while a standard pan is driven. This operation is conducted only once in the production line. The tool

sends the power information to the microcontroller instantly so the microcontroller calibrates itself.

Coming to the issue how the delivered power can be detected, two methods arise: The usage of a current transformer or the usage of a shunt resistor method. The Vestel power boards use the current transformer method. However, the shunt resistor method will also be explained shortly.

*Current Transformer*

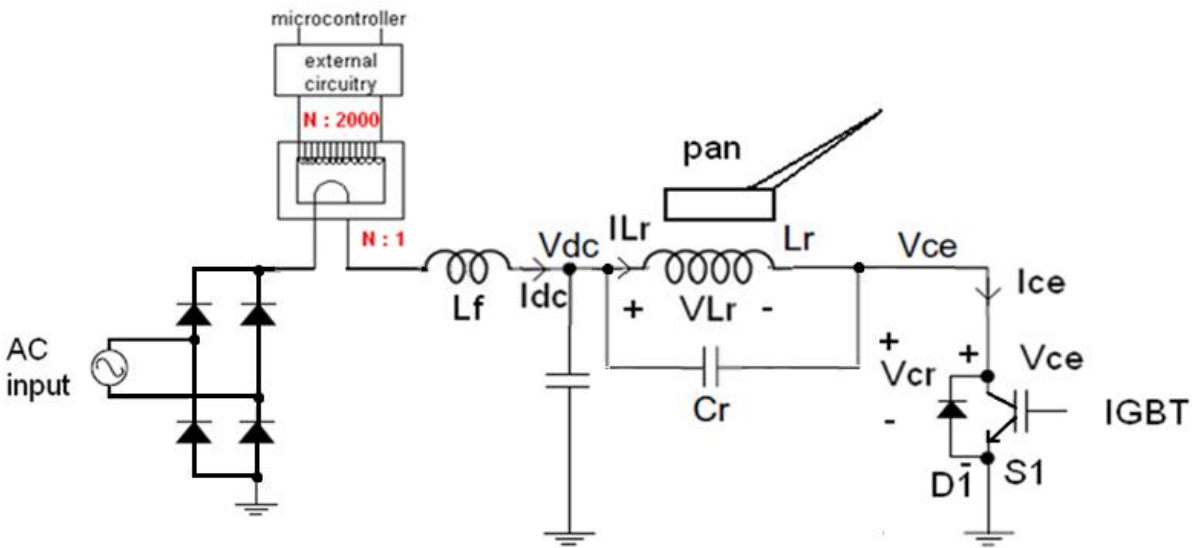


Figure 4.10 Current Transformer

As seen in Figure 4.10, the current transformer is actually a basic transformer with 1 turn of primary and 2000-3000 turns of secondary. Large current (0 -16 A range) flows through the primary however very little amount of voltage (0,002 volts) is induced by the primary to the transformer. Then again very little amount of flux is produced. However, since secondary voltage is the multiplication of primary voltage with turns ratio, a considerable amount of voltage is induced in the secondary (3V-4V). This 3V-4V range is very suitable for the MCU ADC input. The method lets the MCU know the power (current) delivered to the system.



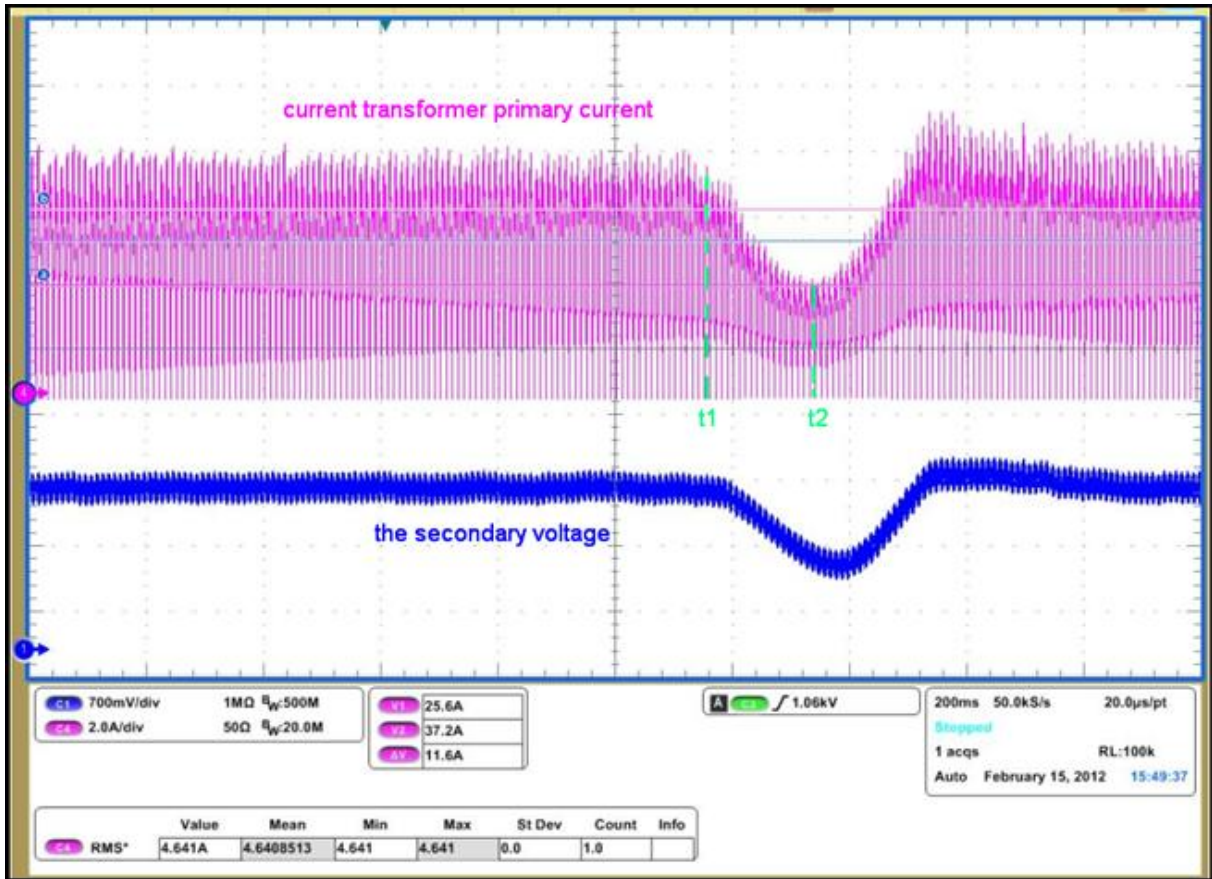


Figure 4.11 Current Transformer Primary Current 2A/div,  
Current Transformer Secondary Voltage 700mV/div

In Figure 4.11, before the instant of t1, the system is driven with 1100W. At the instant t1, the pan is moved on the coil 4-5 cm towards to the out of the coil. So the power delivered decreases to 700W levels. However, the MCU gets this information from the secondary voltage of the current transformer and starts increasing the ON time at the instant t2. The power delivered is again increased to 1100W levels. The only difference is the ON time Intervals.

#### Shunt Resistor

A very small resistance (5-10 milliohms) with high wattage can be placed in series with the IGBT. In this method, the voltage across the resistance must be amplified first. The reason is that, even when peak current passes through, the voltage across the resistor is 0,3 volts peak. With a non-inverting amplifier circuitry, this voltage can be amplified. Moreover, an integrator circuit must be used to get accurate information. The reason is that the voltage across the resistor will be in the shape of current in Figure 4.2 in Chapter 4. In other words, the signal will have an AC shape with a period of 40 $\mu$ S. If this data was entered to the ADC

channel directly, the instants when the data is taken from the signal would be random so inaccurate information would be provided. However, with an integrator circuit, the voltage information over the resistor can be turned into a data for the microcontroller. Then similar algorithms as explained in the Current Transformer part could be applied for this method too.

### 4.3.2 Pan Detection

One of the reasons of high efficiency for induction cookers is the fact that no energy is transferred to the pan in case it is removed. The microcontroller stops driving the IGBTs. Also if the hob is started by the user but there is no pan on the hob, the microcontroller does not start driving the IGBTs. It checks whether a pan is placed or not once every second, which is called pan detection shown in [16].

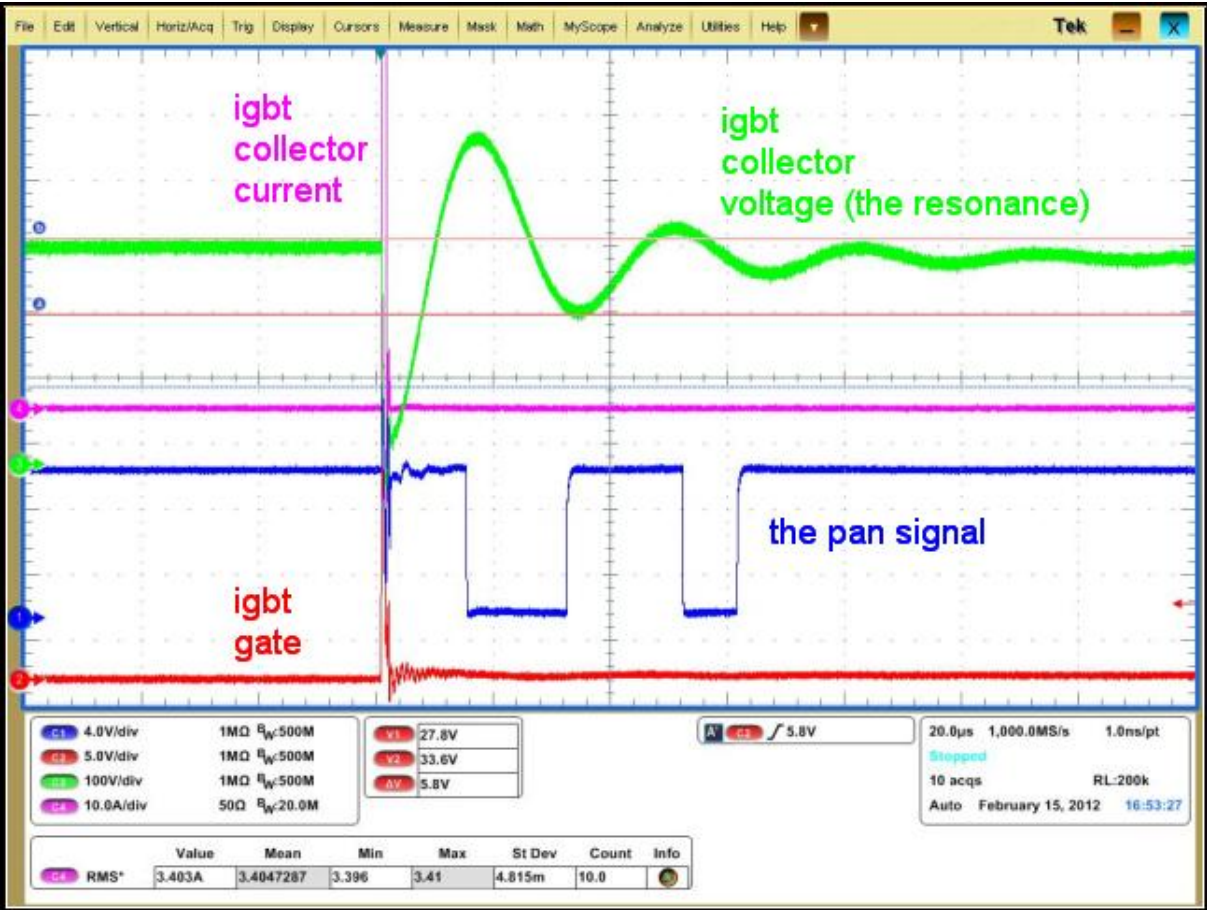


Figure 4.12 IGBT collector voltage ( $V_{CE}$ ) 100V/div, IGBT collector current ( $I_{IGBT}$ ) 10A/div, IGBT gate voltage ( $V_{GE}$ ) 5V/div, Time  $20\mu\text{s}/\text{div}$ , Pan voltage 4V/div in case **there is a ferromagnetic pan**

As seen in Figure 4.12, the MCU sends a very short ON time to the IGBT. During normal driving operation, the on time is around 20 $\mu$ S but in pan detection mode, the on time is 1 $\mu$ S. Since the resonant capacitor is also charged at that instant, when IGBT is shorted for 1 $\mu$ S, the 325Vdc is also shorted to the ground via capacitor. Very high currents pass through the IGBT (100A ranges) at this instant as shown as green in the Figure. This current passes through the capacitor not the coil at this instant since the capacitor is discharged initially. After this 1 $\mu$ S trigger, the resonant capacitor has the voltage of -325Vdc while it had 0 volts just before. (Note that the resonant cap voltage equals to 325Vdc less of IGBT collector voltage shown as purple.)

Then the resonant capacitor immediately starts charging the inductor. The energy transfer is only between the res cap and the res inductor in case of no pan. Then the direction of the current reverses and this time the inductor starts to charge the capacitor. This way the Resonance occurs. “If no pan is placed on the hob, since there is no energy transfer, the resonance would continue for many many cycles theoretically to infinitive. However due to internal losses, the cycles continue for 40-50 times in case of no pan.”

In Figure 4.12, there is a pan on the hob, so the cycles can keep only a few times. The energy is transferred to the pan in this case. The collector voltage over the IGBT (purple) is compared with the Bulk capacitor voltage (325Vdc) by an op-amp comparator and the pan signal is produced by this way.

As seen clearly in Figure 4.12, the IGBT collector voltage is sometimes below the bulk cap voltage sometimes above during the resonance. It was already mentioned that if there is no pan, there would be many cycles of the resonance that would result in many pan signals. The microcontroller counts the number of pan signals and determines whether a pan is placed on the hob or not.

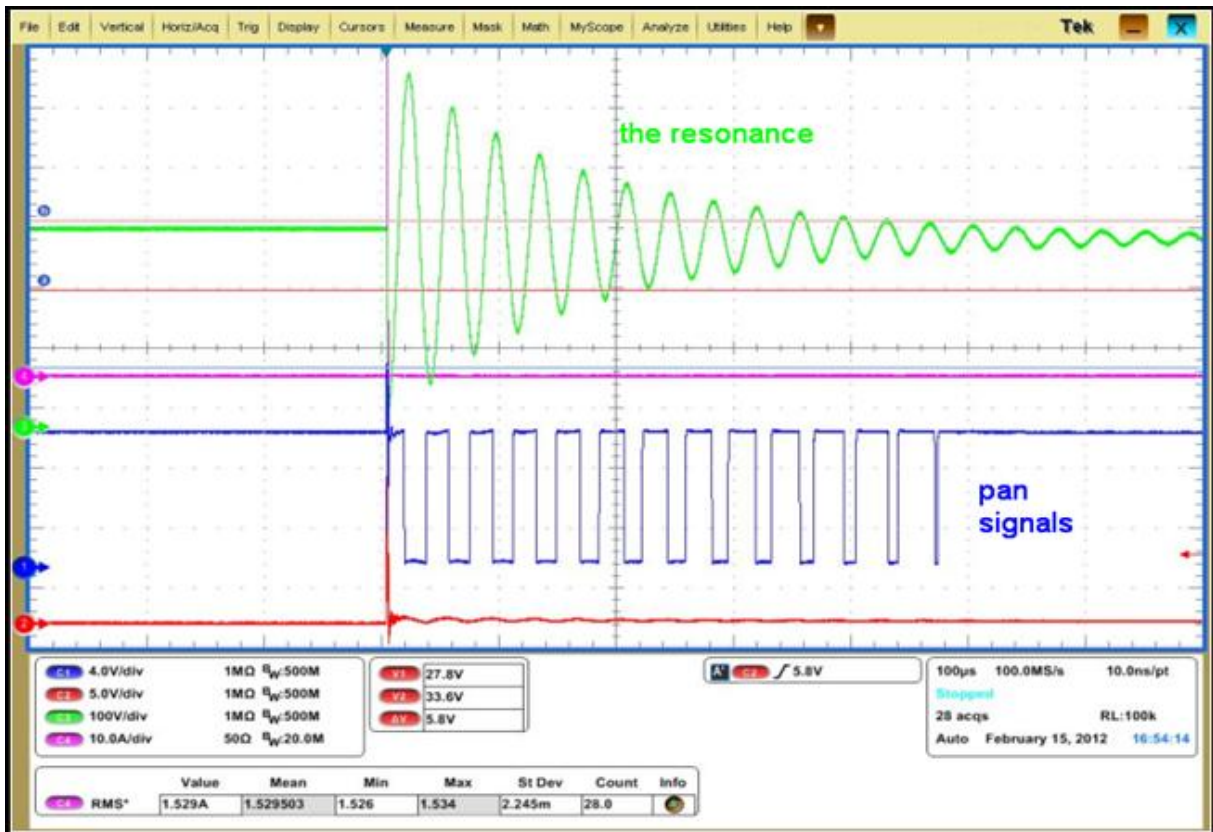


Figure 4.13  $V_{GE}$ ,  $V_{CE}$ , Pan signal in case **there is an aluminum pan**

In Figure 4.13, a much less ferromagnetic pan (aluminum) is placed on the hob. In this case some energy can be transferred to the pan but because of less transfer of energy, the number of cycles can grow up to 13-14. In this case, it is microcontroller's decision to make whether this pan will be authorized to be driven or not. Vestel Induction cooker accepts maximum seven cycles to drive a pan. This system is also used for Minimum Size Detection. Small sizes of ferromagnetic pans act like less ferromagnetic pans. This trigger is repeated once in every second until a pan is placed on the hob. When the cooker detects a pan, it starts to drive it.

### 4.3.3 Protection Circuits

#### *Masking the wrong IGBT turn-on signal*

It is very important not to turn on the IGBT when there is a considerably positive voltage over the IGBT (at the collector). It is important because the switching loss must be minimized to increase performance and reliability. The pan signals which were also shown in Figure 4.12 and 4.13 can be used for this purpose. A more detailed Figure is shown as below in Figure 4.14

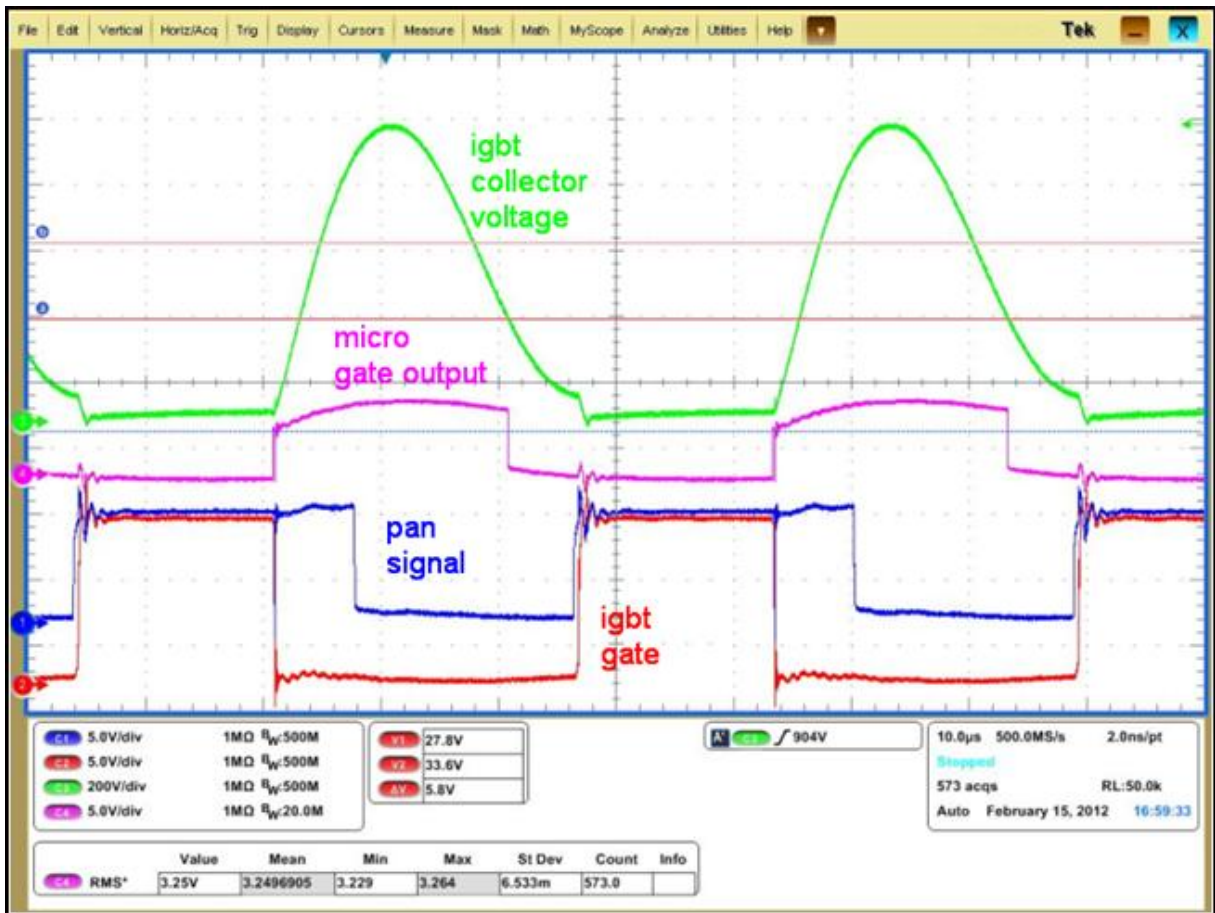


Figure 4.14  $V_{GE}$ ,  $V_{CE}$ , Pan signal, Microcontroller gate during operation

One other reason why the masking is used is that the induction cooker system is a very noisy system. Although, the microcontroller does not tell the IGBT to turn on, some noisy signals can try to turn the IGBT ON. Especially if this wrong signal comes when there is a highly positive voltage (1200 volts) at the collector of the IGBT, the IGBT becomes short-circuited and breaks down directly.

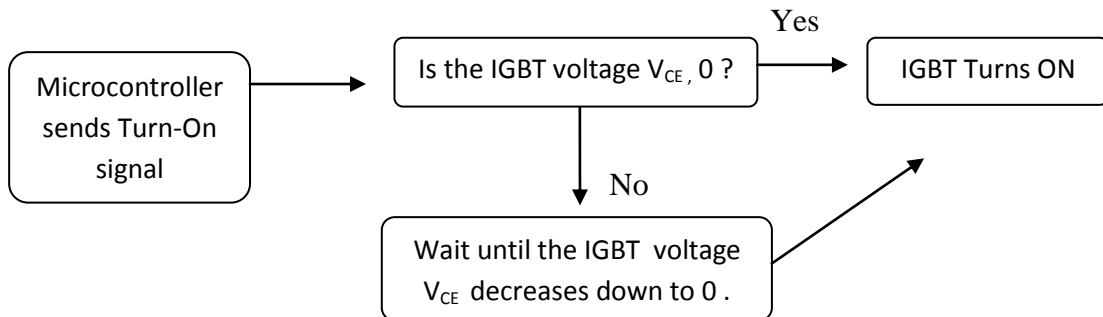


Figure 4.15 IGBT protection algorithm

Because of these two reasons, the IGBT can turn on only in case both the microcontroller and the pan signal allow the IGBT to. As shown in Figure 4.14, when the micro output is high, the IGBT is directly turned off (IGBT gate low). Then the capacitor starts to be charged by the coil and the IGBT collector voltage increases directly. The pan signal which is the comparison result of the IGBT collector voltage and the bulk cap voltage becomes high as the IGBT collector voltage reaches 325Vdc.

After some interval of OFF time ( $\sim 20\mu\text{S}$ ), the microcontroller tells the IGBT to turn ON. However since the collector voltage is still considerably positive, the pan signal does not allow the IGBT to turn ON. As the voltage decreases, the pan signal also allows the IGBT to turn ON. Finally the IGBT is turned ON. Note that the pan signal is reacting after almost  $5\mu\text{s}$  after the exact comparison result. This is achieved by Vestel design by using some external capacitors to provide the delay to the pan signal so that less switching loss is provided.

#### *The Square wave for the Standby*

The electronic board must not drive the IGBTs in case of microcontroller failure or bug cases. Especially in standby mode, the induction cooker must not be turned on in case of miscommunication between the touch-board and the power-board. In other words in case of corrupt data between microcontrollers, the system must still keep in standby mode. If the ON button is pressed for 2 secs, the microcontroller in the touch board tells the microcontroller in the power board to turn on. If this signal was only a TTL Low or High signal, in case of noise or corrupt data, the power boards could wake up unintentionally. To ensure intentional wake up, square wave is sent by the touch board micro to the power board. This square wave turns on the main relay of the system because in stand-by mode, almost all the functions of the power board must be closed for less standby power. Below circuit shown in Figure 4.16 is used for this purpose. The voltage that turns the relay ON becomes TTL High only in case square wave is provided. In case of TTL low or high, the relay cannot turn on.

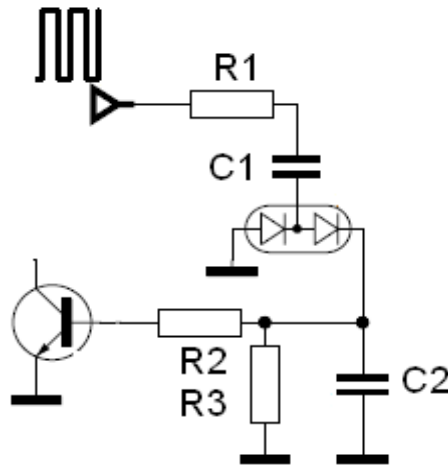


Figure 4.16 The Square Wave

From Standby pin, if TTL High was provided, C1 would be charged directly and become open circuit. So C2 which turns the relay ON would be left discharged. But if square wave is provided, C1 acts like a resistor and C2 is charged through the diodes. The diodes are used to provide the charging current only to the C2 not to Ground. R2 and R3 are to provide reliable BJT turn on. The relay is turned ON if the BJT is ON.

#### *Soft Start*

If the system was to be started directly with the target on and off times, i.e. around 20 $\mu$ S on time 20 $\mu$ S off time, there would be a noisy start up. The reason is that the collector voltage of the IGBT is 325Vdc initially. Note that the voltage at this node is almost 0 during normal switching as the system waits for the resonance to decrease the voltage to 0 volts. So as stated, if directly driven without soft-start, there would be a noisy start-up. So different algorithms can be applied for the best, silent start up. In Vestel design, for 200mS, a constant on time of 1 $\mu$ S is applied then the on-time is increased to the target level step by step as in Figure 4.17.

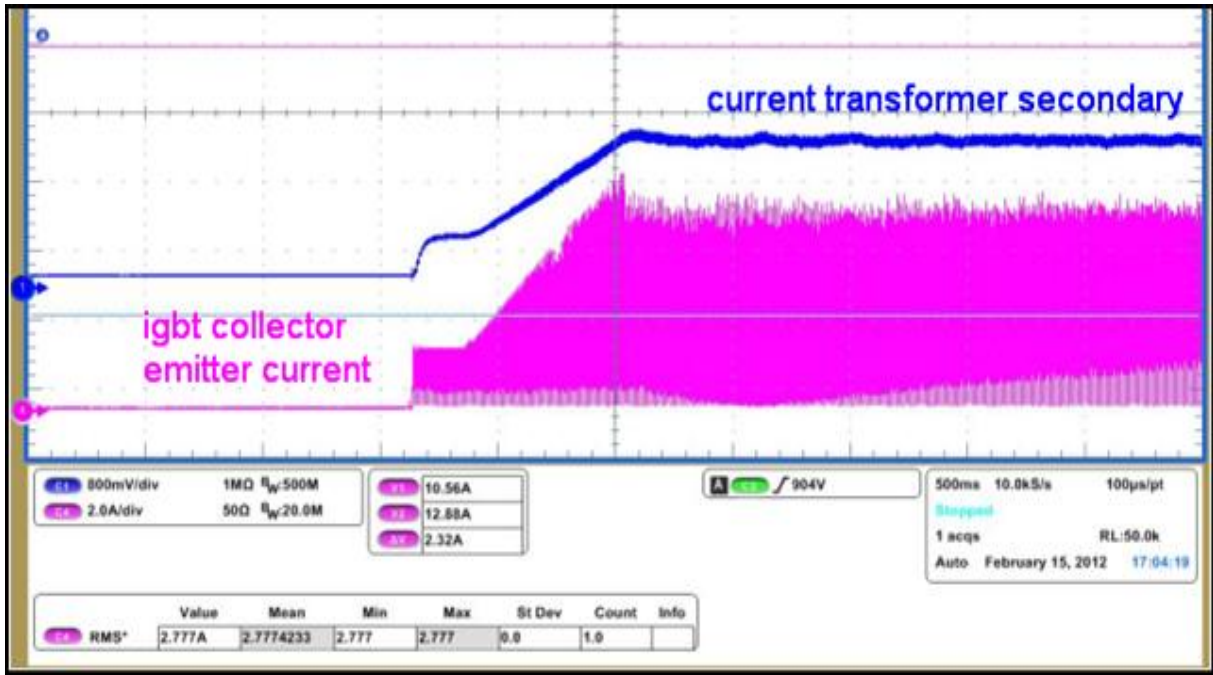


Figure 4.17 Current Transformer voltage during Soft Start

### *Input Voltage Data*

It is also a very important issue not to drive the IGBT close to its maximum drive voltage. If the input voltage increases, the voltage of the IGBT collector also increases during resonance and gets close to the breakdown voltage. So, in order to provide the drive in a safe region, it is a necessary action to decrease the on time if the input voltage increases. This way, the IGBT collector voltage can stay in the same level. The level of the  $V_{ac}$  input voltage can be known by the microcontroller by a simple circuitry if there is no isolation between the primary and the secondary. A simple voltage division after rectification can provide this information. If the primary and the secondary was isolated from each other, more complex circuitry would have to be used which would include opto-couplers or an external transformer. The signal shown in Figure 4.18 enters the ADC input of the microcontroller. The microcontroller takes the average of the signal in every cycle and determines the voltage level.



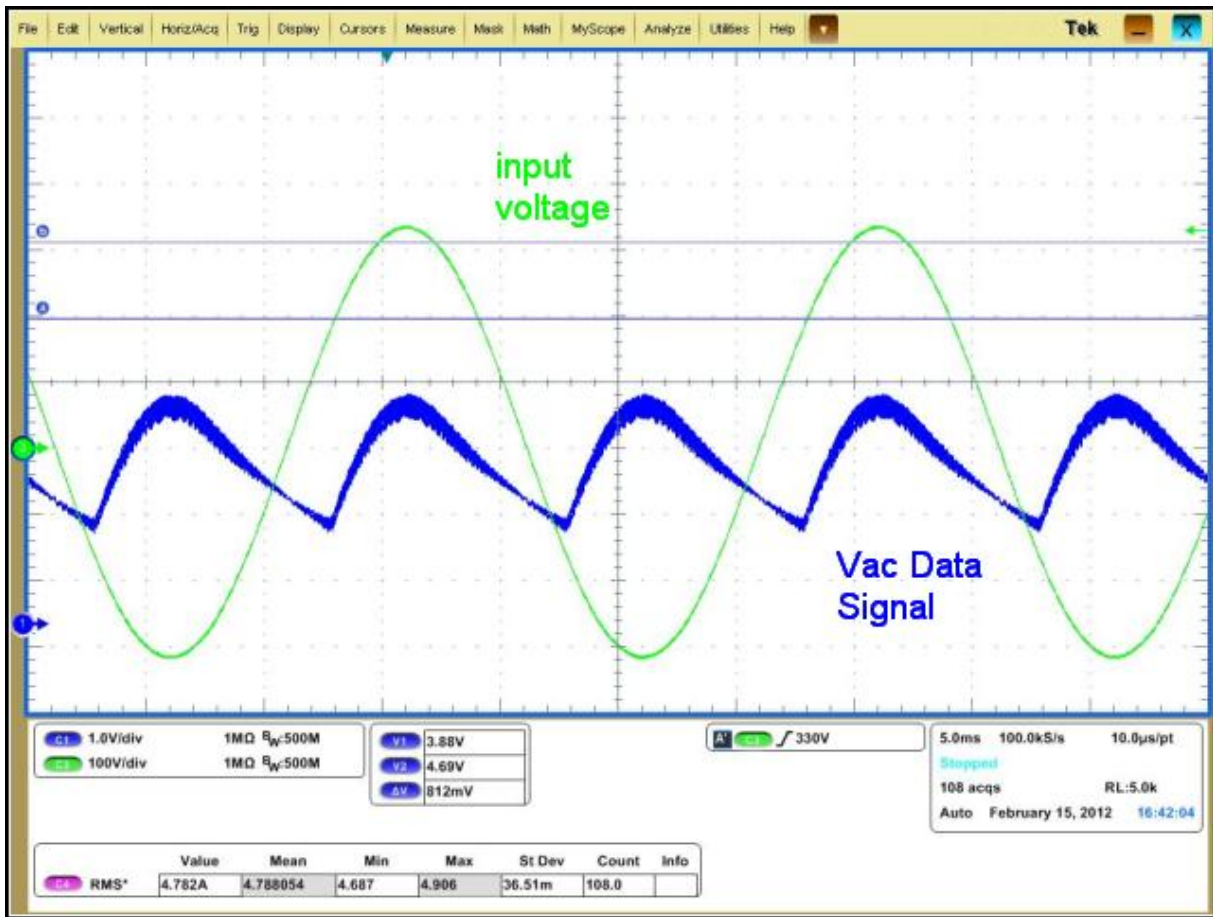


Figure 4.18  $V_{ac}$  Data signal vs input voltage

### Utility Frequency Data

For a reliable induction cooker, the system must know the frequency of the input voltage. There are several reasons for 50Hz information necessity. Firstly, it has been experienced that to start the system drive at the instant of zero cross and to end the system drive again at the instant of zero cross is highly crucial to provide a silent start-up or stop. In other words, to start the drive when there is less energy on the system provides a silent wake-up. Also if the system is not adequate to drive with 60Hz which is a very common frequency in some regions in the world, the frequency data again becomes crucial.

There are many methods to obtain the zero cross information in a system. In Vestel design Induction Cooker, the Line and Neutral are simply compared by an operation amplifier to obtain the data. The advantage of this method is that almost no delay occurs in the measurement of 50Hz while the disadvantage is that additional usage of an op-amp is a cost-up.

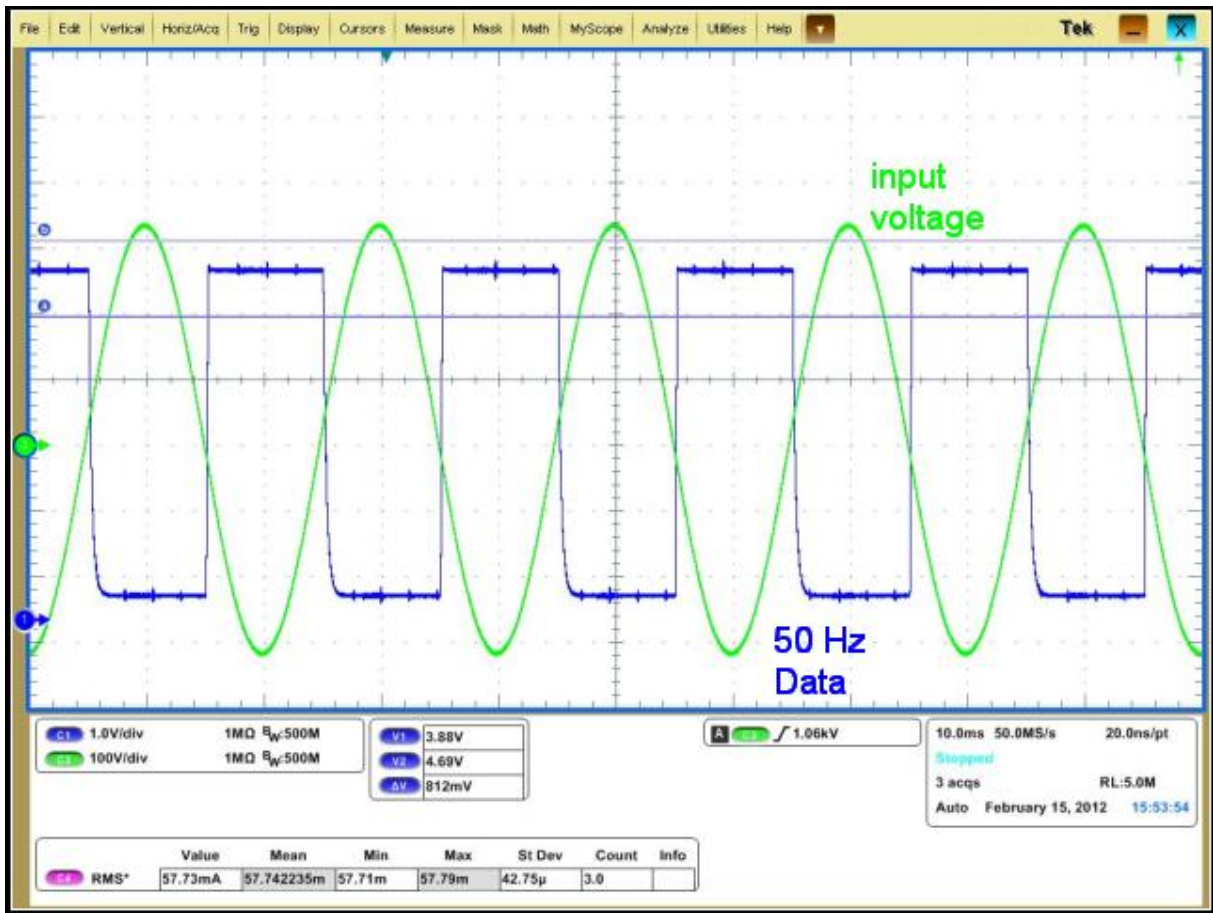


Figure 4.19 50 Hz signal vs input voltage

## CHAPTER V

### CONCLUSIONS and FUTURE WORK

Compared to traditional gas or electric cookers, the importance of induction cooker has increased tremendously because of the dominating factors: Safety, Reliability, Speed and Efficiency. The customer cannot burn his/her hand as there is no direct fire, which is the basic safety advantage. There are many error displays and protective circuits, which make induction cooker reliable. Moreover, since the efficiency is much higher than that of an electric or gas cooker, cooking time has considerably decreased. These are the main reasons why the demand for induction cooker throughout the world is increasing aggressively.

Through this thesis, firstly electromagnetic induction, fundamental theory and the skin effect were covered to point out the basics of an induction cooker system. Then, general block diagram of an induction cooker has been represented to clarify the combination of the system features. Moreover, switching theory as hard and soft switching, the resonant converter analysis and the theoretical analysis of QRT have been covered. Having stated the theoretical results, the thesis expresses the experimental results. A power board with a rating of 2300W that consists of QRT was assembled. Also, control and protection circuits were covered which are the main features of an induction cooker. Lastly, the quasi resonant and the half bridge topologies which can probably be used in an induction cooker were compared theoretically.

If Jitter Method is applied as mentioned in the thesis, IGBT voltage rating reduction is obtained as well as EMI improvement and vibration noise reduction. It was observed that the QRT is more advantageous than half bridge topology when Jitter Method is used to drive the semiconductor switches. The current harmonics that are drawn from the utility are inside the limits of the standard of TS EN 61000-3-2.

As future work, it is planned to design a similar system that can drive up to 3600W for one hob. Most of the design parameters will be updated so that the system can be capable of

driving 3600W safely. Moreover, as it was stated that the use of current transformers made it necessary to calibrate the power levels in production line, it is planned to make an alternative design with shunt resistors for current measurement. The reason is that shunt resistor specifications have much less variations than current transformers.

## BIBLIOGRAPHY

- [1] Renesas Trademark, Induction cooking basics, Aug 2008.
- [2] W.C. Moreland, The induction range: "Its performance and its development problems", *IEEE transactions on industry applications*, vol. IA-9, pp. 81-85, 1973
- [3] Epcos Trademark, Energy efficiency in the kitchen, pp. 1-4, 2008.
- [4] R. Chen, J. Huang, V. Cai, "Induction cooker design with cap-sense", *Cypress*, No: 001-50475, January 2009.
- [5] ST Trademark, A single plate induction cooker with the ST7FLITE09Y0, 2009.
- [6] N. Mohan, Undeland, Robins, *Power electronics converters applications and design*, Wiley, 2003.
- [7] A.D. Pathak, "New optimized IGBTs for induction cooking", *IXYS Corp.*, pp. 37-39, 2007.
- [8] A.K.M. Al-Shaikli, "Analysis of induction cooker coil", *Eng & Tech. Journal*, Vol. 28, 2010.
- [9] S. Moisseev, M. Nakamura, E. Hiraki, H. Omori, H. Yamashita, "Zero voltage soft switching PWM high frequency inverter using IGBTs for induction", *IEE Proceedings, Electric Power Applications*, vol. 150, pp. 237-244, 2003.
- [10] K.H. Liu, R. Origanti, "Resonant switches, topologies and characteristics", *IEEE Power Electronics Specialists Conference*, pp. 106-116, 1985.
- [11] Fairchild Trademark, AN9012 Induction heating system topology overview, 2000.
- [12] H. Omori, H. Yamashita, "A novel type induction heating single ended resonant inverter using new bipolar darlington transistor", *IEEE Power Electronics Specialists Conference*, pp. 590-599, 1985.
- [13] A.S. YIP, "Induction cooking in Hong Kong", *HKECA Journal*, vol. 13, pp. 112-118, 1999.
- [14] Infineon Trademark, Application specific trench-stop IGBT technology for induction cooking, 2011.
- [15] Samsung Trademark, All in one IH cooker, 2010.
- [16] Holtek Trademark, Using the HT45R38 for pan detection in induction cookers, pp.2-3, 2007.

- [17] H.W. Koertzen, J.D.V. Wyk, J.A. Ferreira, “Design of the half bridge series resonant converter for induction heating”, *IEEE Power Electronics Specialists Conference*, vol. 2, pp. 729-736, 1995
- [18] Holtek Trademark, Using the HT46R12A in an induction cooker, pp. 2-11, Jul 2007.
- [19] H.B. Ertan, B. Çolak, “Design issues and a novel approach for measurement and elimination of conducted EMI for an induction cook top”, *International Conference on Electromagnetic Compatibility*, pp. 1-7, 2002.
- [20] TS EN 61000-3-2:2006 Electromagnetic compatibility (EMC) Part 3.2: Limits for harmonic current emissions (equipment input current  $\leq 16$ A per phase).
- [21] D.W. Hart, *Power Electronics*, McGraw-Hill, 2011.
- [22] J. Acero, J.M. Burdio, L.A. Barragan, D. Navarro, “EMI improvements using the switching frequency modulation in a resonant inverter for domestic induction heating appliances”, *35th Annual IEEE Power Electronics Specialists Conference*, pp. 3108-3112, 2004.
- [23] L.A. Barragan, J. Acero, D. Navarro, “FPGA Implementation of a switching frequency modulation circuit for EMI reduction in resonant inverters for induction heating appliances”, *IEEE Transactions on Industrial Electronics*, vol. 25, no. 1, pp. 11-20, 2008.
- [24] D. Gonzalez, J. Balcells, A. Santolaria, “Conducted EMI reduction in power converters by means of periodic switching frequency modulation”, *IEEE Transactions on Power Electronics*, vol. 22, no. 6, pp. 2271-2281, 2007.
- [25] J. Jittakort, S. Chudjuarjeen, “A dual output series resonant inverter with improved assymetrical voltage cancellation control for induction cooking appliance”, *IECON 2011 - 37th Annual Conference on IEEE Industrial Electronics Society*, pp. 2520-2525, 2011.
- [26] A. Jangwanitlert, J. Songboonkaew, P. Chancharoensook, “A modified ZVS flyback resonant inverter for induction cooking applications”, *World Academy of Science, Engineering and Technology*, pp. 261-265, 2008.
- [27] P.Viriya, K. Matsuse, S. Sittichok, “Analysis of high-frequency induction cooker with variable frequency power control”, *Power Conversion Conference*, vol. 3, pp. 1502-1507, 2002.

- [28] T. Nishida, S. Moisseew, E. Hiraki, M. Nakaoka, "Duty cycle controlled soft commutation high frequency inverter for consumer induction cooker and steamer", *Industrial Electronics Society, IECON '03. The 29th Annual Conference of the IEEE*, vol. 2, pp. 1846-1851, 2003.
- [29] J.K. Byun, C. Kyung, H. Song-Yop, "Optimal design procedure for a practical induction heating cooker", *IEEE Transactions on Magnetics*, vol. 36, pp. 1390-1393, 2000.
- [30] P. Achara, P.Viriya, K. Matsuse, "Analysis of a half - bridge inverter for a small-size induction cooker using positive-negative phase-shift control under ZVS and NON-ZVS operation", *PEDS '07. 7th International Conference on Power Electronics and Drive Systems*, pp. 157-163, 2007.
- [31] H. Omori, S. Wang, K. Izaki, H. Yamashita, M. Nakaoka, "Induction-heated cooking appliance using new quasi-resonant ZVS-PWM inverter with power factor correction", *IEEE Transactions on Industry Applications*, vol. 34, pp. 705-712, 1998.
- [32] B.S. Sazak, S. Cetin, S. Oncu, "A simplified procedure for the optimal design of induction cooking appliances", *International Journal on Electronics*, vol. 94, pp. 197-208, 2007.
- [33] V. Crisafulli, C.V. Pastore, "New control method to increase power regulation in a AC/AC quasi resonant converter for high efficiency induction cooker", *3rd IEEE International Symposium on Power Electronics for Distributed Generation Systems (PEDG)*, pp. 628-635, 2012.

## VITA

Mehmet Emin TL was born in 1986 in Isparta, Turkey. He graduated from İzmİr Konak Anatolian High School in 2004 as top student. He ranked 478<sup>th</sup> in “SS” in 2004 in Turkey, while he ranked the 3<sup>rd</sup> in İzmİr Mathematics competition. He received the B.Sc. degree from Middle East Technical University (METU) in Electrical & Electronics Engineering (2004-2009). He worked one year in Arelik and has been working at VESTEL as an R&D engineer for the last two years.